Emission characteristics of reactive organic gases from industrial volatile chemical products (VCPs) in the Pearl River Delta (PRD), China

Sihang Wang[1], Bin Yuan[1,*], Xianjun He[1], Ru Cui[1,a], Xin Song[1], Yubin Chen[1], Caihong Wu[1], Chaomin Wang[1], Yibo Huangfu[1], Xiao-Bing Li[1], Boguang Wang[1], Min Shao[1]

[1] College of Environment and Climate, Institute for Environmental and Climate Research, Guangdong-Hongkong-Macau Joint Laboratory of Collaborative Innovation for Environmental Quality, Jinan University, Guangzhou 511443, China

[a] now at: Nanjing Intelligent Environmental Science and Technology Co.Ltd, Nanjing 211800, China

*Email: byuan@jnu.edu.cn

Abstract:

Volatile chemical products (VCPs) have become an important source of reactive organic gases (ROGs) in urban areas worldwide. Industrial activities can also utilize a large amount of VCPs and emit many organic gases into the atmosphere. Due to multiple sampling and measurement challenges, only a subset of ROG species is usually measured for many industrial VCP sources. This study aimed to investigate the emissions of ROGs from five industrial VCP sources in the Pearl River Delta (PRD) region of China, including shoemaking, plastic surface coating, furniture coating, printing, and ship coating industries. More comprehensive speciation of ROG emissions from these industrial VCP sources was developed by the combination of the proton transfer reaction time-of-flight mass spectrometer (PTR-ToF-MS) along with gas chromatography-mass spectrometer/flame ionization detector (GC-MS/FID). Our study identified oxygenated ROG species (OVOCs) as representative ROGs emitted from these sources, which are highly related to specific chemicals used during the industrial activities. Moreover, mass spectra similarity analysis revealed significant dissimilarities among the ROG emission from industrial activities, indicating substantial variations between different industrial VCP sources. Except for the ship coating industry utilizing solvent-borne coatings, the proportions of OVOCs range from 67% to 96% in total ROG emissions and 72% to 97% in total OH reactivity (OHR) for different industrial sources, while the corresponding contributions of OVOCs in the ship coating industry are only 16%±3.5% and 15%±3.6%. The industrial VCP sources associated with solvent-borne coatings exhibited a higher ozone formation potential (OFP), reaching as high as 5.5 and 2.7 g $O_3 \cdot g^{-1}$ ROGs for ship coating and furniture coating industries, primarily due to contributions from aromatics. We find that a few species can contribute the majority of the ROG emissions, and also their OHR and OFP from various industrial VCP sources. Our results suggest that ROG treatment devices may have limited effectiveness for all ROGs, with treatment efficiencies ranging from -12% to 68%. Furthermore, we found that ambient measurements in industrial areas have been significantly impacted by industrial VCP sources, and ROG pairs (e.g.,

methyl ethyl ketone (MEK) /C_8 aromatics ratio) can be utilized as reliable evidence by using high time-resolution ROG measurements from PTR-ToF-MS. Our study demonstrated the importance of measuring a large number of ROGs using PTR-ToF-MS for characterizing ROG emissions from industrial VCP sources.

1. Introduction

With the successful control of vehicular emissions, emission from volatile chemical products (VCPs) have become an increasingly significant source in cities all around the world (Sun et al., 2018;McDonald et al., 2018;Li et al., 2019;Khare and Gentner, 2018;Seltzer et al., 2022;Sasidharan et al., 2023). Reactive organic gases (ROGs), organic gases other than methane, from VCPs emission can contribute substantially to both anthropogenic secondary organic aerosol (SOA) and ozone (O_3) in urban environments (Seltzer et al., 2022;Khare et al., 2022;Sasidharan et al., 2023;Coggon et al., 2021;Gkatzelis et al., 2021b;Qin et al., 2021). With the development of economy and industrialization, the emissions of industrial VCPs contribute to approximately 25%-45% of ROG emissions in China (Ou et al., 2015;Wei et al., 2011;Huang et al., 2011;Sha et al., 2021;Zhou et al., 2020b). To effectively control atmospheric pollution in urban areas and surrounding regions, it becomes imperative to gain a comprehensive understanding of the emission characteristics of ROGs from industrial VCP sources.

Extensive research has been conducted to investigate ROG emissions from industrial VCP sources, mainly focusing on sampling within manufacturing workshops and exhaust stacks (Zheng et al., 2013;Yuan et al., 2010;Wang et al., 2014). Previous studies have demonstrated that the use of individual chemicals (i.e. coatings, inks, and adhesives) significantly impact ROG emissions (Gkatzelis et al., 2021a;Zheng et al., 2013;He et al., 2022a), and these chemicals used for printing, furniture, and shoemaking industries has seen rapid growth and widespread adoption in recent years (Gkatzelis et al., 2021a;McDonald et al., 2018;Seltzer et al., 2022;Coggon et al., 2021). Consequently, the diverse emission sources and emission factors from industrial VCP sources have contributed to large uncertainties (Mo et al., 2021;Zhong et al., 2018). To mitigate the emissions of most primary pollutants, stricter emission standards have been implemented along with advancements in ROG treatment technologies in China. Specifically, water-borne VCPs has substituted solvent-borne VCPs in several industries, such as printing, interior wall coating, and automotive manufacturing.

However, the replacement in steel structures, automotive plastic parts manufacturing and ship building industries remains below 3% (Mo et al., 2021;Li et al., 2019;Shi et al., 2023;Wang et al., 2023). As a result, the emission characteristics of ROGs from industrial VCP sources may undergo changes in response to the ongoing development of VCPs and ROG treatment technologies. It is imperative to regularly updated the understanding of ROG emission characteristics associated with industrial VCP sources.

The emissions of oxygenated ROG species (OVOCs) have been identified as significant components in industrial VCP emissions (Chang et al., 2022;Mo et al., 2021;Sha et al., 2021). For instance, it has been found that more than 80% of total ROG emissions for shoemaking and printing industries are attributed to OVOC emissions (Zheng et al., 2013). This notable contributions of OVOCs, such as acetone, methyl ethyl ketone (MEK), ethyl acetate, and isopropanol, can be primarily attributed to the use of individual industrial chemicals (Zheng et al., 2013;Wu et al., 2020b). Traditionally, the collection of ROGs involved the use of canisters or Tedlar bags, and their analysis was conducted using gas chromatography-mass spectrometer/flame ionization detector (GC-MS/FID) techniques, with a primary focus on hydrocarbon emissions (Yuan et al., 2010;Wang et al., 2014). Previous studies commonly employed 2,4-dinitrophenylhydrazine (DNPH) cartridges for collection and analyzed them using high-performance liquid chromatography (HPLC) to detect carbonyl species such as aldehydes and ketones. However, this approach is both time-consuming and susceptible to contaminations (Mo et al., 2016;Han et al., 2019).

Due to the intricate chemical compositions of industrial VCPs, it is essential to characterize ROG emissions with higher mass resolution. The proton-transfer-reaction time-of-flight mass spectrometer (PTR-ToF-MS) has been extensively utilized for the identification of VCP sources. More evidence shows that the contribution of VCP sources to anthropogenic ROG emissions is gradually becoming more prominent. For instance, ROG emissions from VCP contribute 50%-80% of anthropogenic ROG emissions in US cities (Gkatzelis et al., 2021b;McDonald et al., 2018). The large fractions (~50%) of ROGs have been attributed to a VCP-dominated source in

Guangzhou, highlighting its importance in urban environments (Li et al., 2022). Through high mass resolution analysis, tracer compounds for various VCP categories have been identified (Gkatzelis et al., 2021a;Coggon et al., 2018;Stockwell et al., 2021). In addition, OVOCs such as acetates, acrylates, alcohols (e.g. benzyl alcohol), glycols (e.g. propylene glycol, ethylene glycol), and glycol ethers, have been found to make significant contributions to VCPs emission (Seltzer et al., 2021;Li and Cocker, 2018;Li et al., 2018;Khare et al., 2022). With the ability to measure whole mass spectra and offer high mass resolution, the PTR-ToF-MS enables more comprehensive detection of a wide range of ROGs (Cappellin et al., 2012;Yuan et al., 2017;Huangfu et al., 2021). By employing parameterization methods to determine instrument sensitivity, more ROGs can be quantified from the obtained mass spectra (Sekimoto et al., 2017;Wu et al., 2020a). Furthermore, previous studies have demonstrated that higher alkanes, including acyclic, cyclic and bicyclic alkanes can be measured using PTR-ToF-MS with NO^+ chemical ionization (NO^+ PTR-ToF-MS) (Inomata et al., 2014;Koss et al., 2016;Wang et al., 2020;Chen et al., 2022). Higher alkanes are significant species in vehicle and combustion emissions (Gao et al., 2023;Liu et al., 2021;Zhao et al., 2018b), and they were not included in previous measurements of industrial VCP sources. Thus, by combining hydrocarbons measured by offline GC-MS/FID, PTR-ToF-MS shows promise as a method for developing more comprehensive speciation relevant to industrial VCP emissions (Gao et al., 2023).

In this study, we applied a PTR-ToF-MS employing H_3O^+ and NO^+ chemical ionization along with a GC-MS/FID to comprehensively measure ROG emissions from five industrial VCP sources, including shoemaking, plastic surface coating, furniture coating, printing, and ship coating industries in the PRD region of China. We investigated emission characteristics of ROGs across these industries, and utilized the dataset to analyze the contributions of different ROG components to total ROG emissions, OH reactivity (OHR), ozone formation potential (OFP), and volatility in various industrial VCP sources. Furthermore, we conducted intercomparisons of the mass spectra characterizations of ROG emissions, which revealed significant variations

in ROG emissions from industrial VCP sources.

2. Materials and methods

2.1 Tested industrial VCP sources and sampling methods

Based on comprehensive analysis of written data, consultation with relevant experts, and thorough on-site investigations, we selected five representative factories and industries from various industrial VCP sources. The selection criteria for these industries were based on relevant emission inventory research conducted in the PRD region of China (Zhong et al., 2018). Sampling methods focused on capturing ROG emissions generated during the main manufacturing processes, such as coatings spraying and adhesives usage in the factories. Both online measurements and offline sampling were carried out in semi-open workshops, as well as ROG treatment devices (i.e. before and after emission treatment, generally located at the front and rear sampling ports of the ROG treatment devices) in the factories (Table. S1).

Typically, workshop waste gases are routed through collection devices (e.g. gas-collecting hoods, airtight partitions), and then processed in ROG treatment devices (e.g. ultraviolet-ray (UV) oxidation, activated carbon adsorption, combustion, and biodegradation). These treated gases are then released into the atmosphere through exhaust stacks. ROG treatment devices play a crucial role in reducing ROG emissions by employing recovery and destruction technologies (Wang et al., 2023;Kamal et al., 2016). Recovery processes involve enriching and separating VOCs by means of temperature or pressure changes and selective absorbents, while destruction processes converts VOCs into harmless substances such as CO_2 and H_2O through combustion (Wang et al., 2023). In this study, we evaluate two types of ROG treatment devices: activated carbon adsorption combined with UV photolysis devices (installed in shoemaking, plastic surface coating, furniture coating, and printing industries) and catalytic combustion devices (installed in printing and ship coating industries).

During the campaign, a mobile monitoring vehicle was equipped with online measurement equipment and strategically parked near the sampling ports of both workshops and ROG treatment devices emissions (Fig. S1). A CO_2 / H_2O gas analyzer

(LI-COR 840A, Inc., USA) was used to measure the concentrations of CO_2 and H_2O. To ensure continuous sampling, air from various factories was drawn through a length of Perfluoroalkoxy (PFA) Teflon tubing, ranging from 10 to 100 meters, at a controlled flow rate of 6 L/min facilitated by an external pump. The use of long tubing was assessed through laboratory tests, which showed that the tubing had a negligible and minor influence on most ROG species. This confirmed the feasibility of measurement using long PFA tubing, more detail can be found elsewhere (Li et al., 2023).

2.2 ROG measurements

In this study, ROG were measured using a proton transfer reaction quadrupole interface time-of-flight mass spectrometer (PTR-QiToF-MS) (IONICON Analytik, Innsbruck, Austria) (Sulzer et al., 2014) and a combination of canister sampling and offline GC-MS/FID analysis system (canister-GC-MS/FID). More comprehensive speciation of ROG was achieved by analyzing hydrocarbons by canister-GC-MS/FID, quantifying all signals using H_3O^+ PTR-ToF-MS, and supplementing by acyclic, cyclic, and bicyclic alkanes from NO^+ ionization of PTR-ToF-MS. The selection of overlapping ROGs was similar to a previous study (Table. S2) (Gao et al., 2023).

To capture the real-time emission characteristics of ROGs from industrial VCP sources, the mass spectra of PTR-ToF-MS was recorded every 10 s. Prior to each test, background measurements of the instrument were carried out by passing sampling air through a custom-built platinum catalytical converter that had been preheated to 365 °C for 1 minute. Throughout the campaign, the PTR-ToF-MS instrument automatically alternated between two reagent ions (H_3O^+ and NO^+) every 10 minutes. Detailed setting parameters for H_3O^+ and NO^+ chemical modes in this instrument can be found in previous studies (Wu et al., 2020a;Wang et al., 2020;He et al., 2022b). The Tofware software package (version 3.0.3, Tofwerk AG, Switzerland) was employed to facilitate accurate data analysis (Stark et al., 2015).

Calibration for ROGs measure by PTR-ToF-MS were carried out both in the laboratory and during the campaign. The PTR-ToF-MS was regularly calibrated using a 23-component gas standard (Linde Spectra) throughout the campaign. During the later

period of the campaign, two gas standards (Apel Riemer Environmental Inc.) were used for the calibration of other ROGs, specifically for acyclic and cyclic alkanes using NO^+ chemical ionization. (Wang et al., 2020;Chen et al., 2022;Wang et al., 2022). A total of 11 organic acids and nitrogen-containing compounds were calibrated using the liquid calibration unit (LCU, IONICON Analytik, Innsbruck, Austria) (Table. S3-S5). In order to account for the humidity dependence of some ROGs in the PTR-ToF-MS (Yuan et al., 2017;Koss et al., 2018), humidity-dependence curves established in the laboratory were utilized for correction (Wu et al., 2020a;He et al., 2022b;Wang et al., 2022). Sensitivities of uncalibrated species were determined based on the kinetics of proton-transfer reactions of H_3O^+ with ROGs (Fig. S2) (Cappellin et al., 2012;Sekimoto et al., 2017), with an associated uncertainty of approximately 50% for the concentrations of uncalibrated species.

Simultaneously, offline sampling was conducted near the sampling ports of workshops and ROG treatment devices. Whole air samples were collected using canisters for determination of hydrocarbons in industrial VCP sources, and analyzed by an offline GC-MS/FID system. The GC-MS/FID system was calibrated using photochemical assessment monitoring stations (PAMS) and TO-15 standard mixtures, which enabled the identification and quantification of a total of 94 hydrocarbons. More information about this instrument and dataset for canister sampling and offline GC-MS/FID system can be found elsewhere (Li et al., 2020).

2.3 Calibrations of esters and isopropanol based on H_3O^+ and NO^+ ionization

Since ester species (including acetates and acrylates) play a significant role in industrial VCP sources, it is important to accurately quantify their concentrations (Khare et al., 2022). Previous studies have demonstrated that ethyl acetate exhibits notable fragmentation, resulting in interference at m/z 61 (e.g. $C_2H_4O_2H^+$) and m/z 43 (e.g. $C_2H_2OH^+$) (Haase et al., 2012;de Gouw and Warneke, 2007;Rogers et al., 2006;Fortner et al., 2009). Therefore, we employed the PTR-ToF-MS to directly measure high-purity ester chemicals and identify the characteristic product ions

produced by esters under H_3O^+ and NO^+ chemical ionization. Several common esters including methyl acetate, ethyl acetate, isopropyl acetate, and vinyl acetate, were selected to investigate instrument fragmentation under different ionizations. As shown in Table. S6, it is intriguing to observe that high-molecular-weight acetates tent to exhibit more fragmentation, resulting in interference at m/z 61 (e.g. $C_2H_4O_2H^+$) and m/z 43 (e.g. $C_2H_2OH^+$). Methyl acetate (95%) and ethyl acetate (72%) displayed limited fragmentation in the instrument, while isopropyl acetate accounted for only 13% of the $C_5H_{10}O_2H^+$ ions. Additionally, esters with different chemical structures may undergo distinct modes of fragmentation. For example, vinyl acetate primarily fragmented to produce interfering fragments at m/z 43 (e.g. $C_2H_2OH^+$) with a fraction of 78%. Furthermore, considering the PTR-ToF-MS mass spectra from various industrial VCP sources, it is conceivable that other ester compounds might also contribute to these mass channels, emphasizing the need for cautious consideration of m/z 61 (e.g. $C_2H_4O_2H^+$) and m/z 43 (e.g. $C_2H_2OH^+$) signals measured by H_3O^+ PTR-ToF-MS in industrial VCP sources. The use of NO^+ chemical ionization exhibits various reaction pathways with ROGs (Wang et al., 2020;Chen et al., 2022), which can partially mitigate interference from fragment ions (Table. S6). The identified results of acetates based on NO^+ ionization demonstrated considerable improvements for methyl acetate (83%) and ethyl acetate (80%), whereas vinyl acetate exhibited more fragmentation, with the largest contribution (47%) at m/z 43 (e.g. $C_2H_2OH^+$).

Additionally, it is challenging to calibrate isopropanol in the H_3O^+ PTR-ToF-MS since alcohols split off water during ionization (Buhr et al., 2002). To overcome this challenge, we implemented daily calibrations of isopropanol under ambient humidity conditions throughout the campaign (Fig. S3). The NO^+ PTR-ToF-MS was also employed to calibrate isopropanol by identifying the characteristic product ions produced under NO^+ ionization (Table. S6). The dominating product ion of isopropanol was observed at m/z 59 (e.g. $C_3H_7O^+$) (88%), which corresponds to acetone ($C_3H_6OH^+$) ions in the H_3O^+ PTR-ToF-MS. Although the dominant product ion for acetone under NO^+ ionization was observed at m/z 88 (e.g. $C_3H_6O(NO)^+$) (77%), the interfere at m/z

59 (e.g.$C_3H_6OH^+$) (23%) was not insignificant. Therefore, the concentration of isopropanol measured by NO^+ PTR-ToF-MS in this campaign has eliminated the influence of acetone. Finally, the comparison between PTR-ToF-MS with H_3O^+ and NO^+ chemical ionization is shown in Fig. S4-S5. Previous studies have shown good agreement between measurements obtained using PTR-ToF-MS with H_3O^+ and NO^+ chemical ionization in ambient measurements (Wang et al., 2020). However, a slightly weaker correlation was observed in industrial VCP sources, potentially due to the large changes for different species between the switch of the two reagent ions. Our results demonstrated that the NO^+ PTR-ToF-MS can also provide a complementary approach for characterizing ester species and isopropanol in ambient air as well as emission sources.

2.4 Mass spectra similarity analysis

We conducted a comprehensive comparison of various ROG emission sources by considering the entire range of species in mass spectra as dimensions in a vector, and calculating the cosine angle (θ) similarity (Humes et al., 2022;Ulbrich et al., 2009;Kostenidou et al., 2009). The angle θ between the two mass spectra (MS_a and MS_b) is given by the following:

$$cos\,\theta = \frac{MS_a MS_b}{|MS_a||MS_b|} \quad (1)$$

The θ angles between two mass spectra is divided into 4 groups, including 0°-15°, 15°-30°, 30°-50°, and>50°, which correspond to excellent consistency, good consistency, many similarities, and poor consistency, respectively. Due to the distinct ionization methods of the instruments, our classification of angle similarity is not as strict as that reported in previous studies (Kostenidou et al., 2009;Zhu et al., 2021). As these previous studies utilize the similarity analysis on mass spectra of aerosol mass spectrometer (AMS) obtained from electron ionization, leading to very similar mass spectra for different sources.

3. Results and discussions

3.1 Time-resolved ROG emissions from industrial VCP sources

Time series of several ROGs measured by the H_3O^+ PTR-ToF-MS from five industrial VCP sources are shown in Fig. 1 and Fig. S6. More information for these sources can be found in Sect. S1 in the Supplement. Online measurements were carried out in semi-open workshops (workshops emission) and from ROG treatment devices (i.e. before and after treatment emission). As the waste gas was directly discharged into the ambient air from exhaust stacks, the after treatment emission was can be considered as stack emission (Zheng et al., 2013). The average concentrations of eight representative ROGs, including aromatics, ketones, alcohols, and esters, between workshops emission and stack emission for all factories is presented in Fig. S7. The evaluation of the ROGs treatment efficiency is based on the analysis of emission characteristics before and after treatment in the ROG treatment devices, which is discussed in greater detail in Section 3.3. Along with the typical ROGs, the PTR-ToF-MS measured a wide range of ions in abundance in the mass spectra. Fig. 2 displays mass spectra representing the average concentrations of stack emissions from five industrial VCP sources for all detected ROGs. These ROGs measured by the PTR-ToF-MS were categorized based on their chemical formula, namely hydrocarbon species (C_xH_y), OVOCs ($C_xH_yO_1$, $C_xH_yO_2$, and $C_xH_yO_{\geq 3}$), species containing nitrogen and/or sulfur atoms (N/S-containing), species containing siloxanes (Si-containing), and other ions (others).

3.1.1 Emission characteristics from industrial VCP sources

A. Shoemaking industry

Real-time concentrations of toluene, acetone, ethyl acetate, and isopropanol from the shoemaking industry are displayed in Fig. 1a. The variable manufacturing processes conditions are demonstrated by inconsistent emission levels in the workshops. This variation may be attributed to different emission intensities during different periods. Notably, the significant emissions from the shoemaking industry are primarily attributed to a few low-molecular-weight OVOCs (Fig. 2a), including acetone, MEK, isopropanol, and formaldehyde, followed by a fraction of hydrocarbon species (e.g. toluene). Our results align with previous findings (Zheng et al., 2013;Zhao et al., 2018a),

emphasizing that raw chemicals used during the industrial activities play crucial roles in determining the constituents of the industrial VCP emissions.

B. Plastic surface coating industry

Significant variations in ROG concentrations were also observed from the plastic surface coating industry (Fig. 1b). These variations could be attributed to different manufacturing process conditions and the use of different chemicals in workshops as well. As shown in Fig. 2b, OVOCs contribute significantly to emissions from this industry. Representative OVOCs for $C_xH_yO_1$ ions consist of isopropanol, acetone, formaldehyde, methanol, and cyclohexanone. $C_xH_yO_2$ ions refer to acetates and acrylates such as $C_3H_6O_2$ (e.g. methyl acetate), $C_6H_{12}O_2$ (e.g. butyl acetate), $C_9H_{16}O_2$ (e.g. allyl hexanoate) and $C_{12}H_{20}O_2$ (e.g. linalyl acetate). Notably, there are some differences from the main components compared to previous results (Zhong et al., 2017), which may be attributed to the substitution of solvent-borne chemicals with water-borne chemicals in industrial VCPs.

C. Furniture coating industry

Due to the wide variety of industrial coatings used in the furniture coating industry, numerous ROGs can be observed in the measured mass spectra (Fig. 2c). Notably, $C_xH_yO_2$ (24%) and $C_xH_yO_3$ ions (9%) contribute significantly in this industry. Among the identified species, C_8 aromatics exhibit the highest concentrations, consistent with previous research from industries utilizing solvent-borne coatings (Yuan et al., 2010;Wu et al., 2020b;Wang et al., 2014). Other OVOCs such as MEK, ethanol, and formaldehyde for $C_xH_yO_1$ ions, $C_6H_{12}O_2$ (e.g. butyl acetate), $C_5H_8O_2$ (e.g. methyl methacrylate, acetylacetone) for $C_xH_yO_2$ ions, and $C_6H_{12}O_3$ (e.g. propylene glycol methyl ether acetate, PGMEA) and $C_7H_{14}O_3$ (e.g. butyl lactate) for $C_xH_yO_3$ ions had been found may be associated with emissions from water-borne coatings. This finding underscores the importance of considering high-molecular-weight OVOCs in this industry, further emphasizing the ability of PTR-ToF-MS to better characterize these important OVOCs that serve as raw chemicals for industrial VCPs.

Moreover, by employing online PTR-ToF-MS technology, we can gain deeper

insights into the emission characteristics of ROGs during both working and non-working hours. We conducted an analysis of ROG emissions in the furniture coating factory during non-working hours (from 10:00 p.m. to 8:00 a.m. the next day) and compared them with emissions during working hours (Fig. 1c). Most ROGs exhibited a gradual decrease in concentration during non-working hours, with the exception of formaldehyde which maintained a constant concentration. Notably, the concentrations of other typical ROGs, such as MEK and C_8 aromatics, were 2-5 times lower during non-working hours compared to working hours. This observation suggests that ROGs may still be emitted even when the painting activities in the factory is halted, with night-time emissions accounting for approximately 20% of total daily emissions. The θ angles of mass spectra between real-time concentrations versus working hours shows that ROG emissions have many similarities during both working and non-working hours (Fig. 1d, θ<30° in most times). Additionally, the poor similarity observed between real-time concentrations in workshops during non-working hours and those in the outside air suggests that outside air has minimal influence on ROG emissions during non-working hours (Fig. S8). Given that some ROGs were still more abundant and continued to be released into the atmosphere even during non-working hours (e.g. from the volatilization of chemicals), the ROG emissions in factories during non-working hours should not be ignored.

D. Printing industry

The real-time concentrations of typical ROGs measured from the printing industry is shown in Fig. S6a, with an emphasize on the performance of two different ROG treatment devices, namely activated carbon adsorption combined with ultraviolet-ray (UV) photolysis devices and catalytic combustion devices (specifically, regenerative thermal oxidizer (RTO) devices) installed in this factory. Isopropanol was found to have the highest concentration in the printing industry (Fig. 2d), which is consistent with previous studies (Zheng et al., 2013). The higher concentrations of other typical species, such as $C_4H_8O_2$ (e.g. ethyl acetate), $C_5H_{10}O_2$ (e.g. isopropyl acetate), and $C_7H_{16}O_3$ (e.g. dipropylene glycol methyl ether, DPM) substantiate the correlation

between ROG emissions and industrial inks utilized in the printing industry. It was found that ROG treatment devices exhibit varying treatment efficiencies for ROGs, particularly for OVOCs (such as isopropanol and ethanol), that may not have been effectively removed by these treatment devices.

E. Ship coating industry

In comparison to other industrial VCP sources, the ship coating industry exhibits the highest emissions of hydrocarbons (86%), specifically C_6-C_{11} aromatics (Fig. 2e, also in Fig. S6b, Sect. S1). This may be attributed to the utilization of solvent-borne industrial coatings for ship coating remains prevalent due to stringent requirements for anti-rust and anti-corrosion properties (Malherbe and Mandin, 2007). A few OVOCs, such as methanol and MEK, were identified as significant emissions. These results confirm that ROG emissions from solvent-borne coatings, predominantly composed of C_8 aromatics, continue to be the primary contributors in the ship coating industry, which is consistent with a previous study conducted in the PRD region (Zhong et al., 2017).

3.1.2 Comparison of ROG composition from industrial VCP sources

The quantification of the proportions of different ion categories measured by the PTR-ToF-MS across various industrial VCP sources is shown in Fig.2 and Fig. S9. OVOCs make up the largest fractions in the printing (94%), plastic surface coating (90%), shoemaking (84%), and furniture coating (68%) industries, while they only account for 13% of emissions from the ship coating industry. The fractions of different OVOC groups exhibit a general decline from $C_xH_yO_1$ to $C_xH_yO_{\geq 3}$, and OVOCs with more than two oxygen atoms are present in small proportions (0.3%-8.5%) in all industrial VCP sources except for the furniture coating industry (33%), indicating little emissions of these species. However, although these OVOCs with two or more oxygen atoms do not contribute significantly to the overall emissions, some of them may serve as tracer compounds for particular emission sources as they were only detected in single source. Previous studies have identified octamethylcyclotetrasiloxane (D_4 siloxane), texanol ($C_{12}H_{24}O_3$) and para-chlorobenzotrifluoride (PCBTF, $C_7H_4ClF_3$) as tracer compounds for individual chemicals (adhesives and coatings) in U.S. cities (Gkatzelis

et al., 2021a). We also observed that the concentrations of texanol and PCBTF emitted by relevant industrial VCP sources were unique and almost non-existent in other sources. Texanol was only detected in samples from the plastic surface coating and furniture coating industries that utilize water-borne coatings. Similarly, PCBTF was only found in samples from the ship coating and furniture coating industries that use solvent-borne coatings. These findings suggest that texanol and PCBTF may be applicable as tracer compounds for industrial VCPs in China. On the contrary, D_4 siloxane was not found to be specific to emissions from adhesive-related industrial (i.e. shoemaking industry) (Fig. 2), indicating that D_4 siloxane may not be an appropriate tracer compounds for identifying industrial VCPs in China.

3.2 Distributions of ROG emissions, OHR, OFP, and volatility

We compared the mass spectra of these industrial VCP sources and calculating the θ angles similarity (Fig. 3) (Table. S7). The ROGs showed a diverse similarity among different types of industrial VCP sources. Only plastic surface coating industry versus printing industry demonstrated good consistency (27°), other mass spectra exhibited poor consistency (θ>60°). Combined with mass spectra of vehicular emissions (Wang et al., 2022), the θ angle similarities among the mass spectra of industrial VCP sources (62°-90°) were worse than those of vehicular emissions (41°-75°) (Fig. 3). It is interesting to observe that the θ angle similarity among the mass spectra in different workshops in printing and ship coating industries ranged from1.6° to 9.0° (Table. S8), similar to the mass spectra in various emission standards for gasoline vehicles (4.9°-17°) (Table. S9). Conversely, the θ angle similarity among the mass spectra of workshops in other industrial VCP sources ranged from 13° to 60°, indicating significant differences in ROG emissions from industrial VCP sources. These substantial differences indicate that ROG emissions from industrial VCPs are more complex and diverse than vehicular emissions. Consequently, a more accurate classification of industrial VCP emissions is necessary, as they cannot be directly unified as a single class of emission sources.

The combination of PTR-ToF-MS and canister-GC-MS/FID measurements

allowed for more comprehensive speciation of ROG emissions from industrial VCP sources. This comprehensive approach enabled the determination of the fractions of ROGs in total ROG emissions for various industrial VCP sources (Table. S10, Fig. S5, details in Sect. S2 in the Supplement). Additionally, ROGs reactivity plays a crucial role in characterizing the contributions of different ROGs to atmospheric chemical reactions and the formation of secondary pollutants (Wu et al., 2020a;Yang et al., 2016). The overall OHR of ROGs was calculated to comprehend the role of ROGs emitted by industrial VCP sources. The calculation only employed ROGs with known reaction rate constants with the OH radical, which were taken from previous studies (Atkinson and Arey, 2003;Atkinson et al., 2004;Atkinson et al., 2006;Koss et al., 2018;Wu et al., 2020a;Zhao et al., 2016). The fractions of ROGs in the total OHR of ROGs can be determined for various industrial VCP sources (Table. S11). ROGs are grouped into categories, including OVOCs, N/S-containing, and heavy aromatics and monoterpenes measured by H_3O^+ PTR-ToF-MS, higher alkanes (including C_{10}-C_{20} acyclic, cyclic, and bicyclic cycloalkanes) measured by NO^+ PTR-ToF-MS, and alkanes, alkenes, aromatics, and halohydrocarbons measured by canister-GC-MS/FID.

OVOCs contributed significantly to total ROG emissions (Fig. 4a), and fractions of OVOCs in total ROG emissions are comparable to previous studies (Fig. 5). Notably, OVOCs account for 67% of total ROG emissions from the shoemaking industry, which is slightly lower than findings from other studies in the PRD region (Zheng et al., 2013) but higher than those reported in previous studies (Zhou et al., 2020a;Zhao et al., 2018a). The fractions of OVOCs in total ROG emissions from plastic surface coating, printing, and furniture coating industries are 96%±0.2%, 85%±6.5%, and 77%, respectively. Compared to previous studies (Zhong et al., 2017;Zheng et al., 2013;Fang et al., 2019;Zhao et al., 2018a;Wang et al., 2019;Zhou et al., 2020a;Zhao et al., 2021), determined OVOC fractions for these industrial VCP sources are much higher (Fig. 5), which may be related to two reasons: (1) more OVOC species are detected in this study; (2) water-borne coatings and inks are more widely employed in the recent year which may enhance OVOC fractions. Moreover, OVOCs account for 16%±3.5% of total ROG

emissions from the ship coating industry by using the solvent-borne coatings, and the fraction is also higher than findings from one previous study (Zhong et al., 2017). Additionally, OVOCs also contribute to the largest fraction in total OHR of ROGs from all industrial VCP sources (72%-97%) except for the ship coating industry (15%±3.6%) (Fig. 4b). In contrast to the important contribution of OVOCs, the fractions of hydrocarbons measured by canister-GC-MS/FID only made considerable contributions in specific industrial VCP sources (Fig. 4). For instance, aromatics were found to be the major contributors to both total ROG emissions and OHR in the ship coating industry, making up 74%±6.1% and 79%±4.8% respectively. Alkanes measured by canister-GC-MS/FID only make contributions in the shoemaking industry, comprising 26% of the total ROG emissions. Overall, the total OHR of ROGs was dominated by OVOCs and aromatics, and the contributions of other species were in the range of 1.8%-21% (Fig. 4b). These results stress the importance of measuring a broad range of OVOCs using PTR-ToF-MS in characterizing ROG emissions from industrial VCP sources.

The application of NO^+ PTR-ToF-MS provided the opportunity for detecting emissions of higher alkanes from industrial VCP sources. We show that the contribution of higher alkanes can be significant for VCP sources. Specifically, the printing industry demonstrates a noteworthy presence of higher alkanes, accounting for 27%±2.7% and 8.2%±2.4% in workshop and stack emissions, respectively (Table. S10). This can be attributed to the use of lubricating oil, a primary component of industrial inks, which contains substantial amounts of alkanes (Liang et al., 2018). Furthermore, emissions from forklifts transporting products in printing workshops also contribute to the emission of higher alkanes (Li et al., 2021), suggesting non-road vehicles may contribute to the emissions from industrial VCP factories. In addition, the fractions of higher alkanes in stack emission are lower than in workshops, suggesting that ROG treatment devices effectively reduce emissions of higher alkanes.

To facilitate for making controlling strategies of ozone, we determine the OFP from a unity of emission from different sources for comparison (Yuan et al., 2010;Na and Pyo Kim, 2007), which represent the ability to ozone formation from ROG sources

on a relative basis (Fig. 6), and calculated using the following equation:

$$OFP_i = \sum_{j=1}^{n} f_{ji} MIR_j \quad (2)$$

Where OFP_i is the estimated ozone formation amount when 1 g ROG is emitted from source i, f_{ji} is the mass fraction of species j in source i, and MIR_j is the maximum incremental reactivity (MIR) of species j (Carter, 2007). Among the industrial VCP sources considered, the ship coating industry exhibited the highest OFP, reaching as high as 5.5 g $O_3 \cdot g^{-1}$ ROGs, followed by the furniture coating industry, with a value of 2.7 g $O_3 \cdot g^{-1}$ ROGs. The OFP for other industrial VCP sources ranged from 0.79 g $O_3 \cdot g^{-1}$ ROGs to1.4 g $O_3 \cdot g^{-1}$ ROGs. Among all industrial VCP sources, aromatics (ranging from 4.2% to 91%) and OVOCs (ranging from 6.7% to 94%) were identified as the primary contributors to OFP. Compared to vehicular emissions, the OFP from the ship coating and furniture coating industries are significantly higher (Fig. 6), suggesting that these sources should be controlled in priority. Given the higher reactivity value for ship coating industry relative to other sources, it is evident that controlling ROG emissions from solvent-borne industrial chemicals would have a more substantial impact on reducing ozone formation compared to other sources. Moreover, it is important to note that the emissions of solvent-borne chemicals surpass those of vehicles, while water-borne chemicals have lower emissions compared to vehicles. This observation implies that the substitution of solvent-borne chemicals with water-borne chemicals in China holds considerable importance in mitigating and controlling ozone pollution.

We further compare centralization for species among different ROGs sources by determining the contribution from the top ten species in terms of concentrations, OHR, and OFP (Fig. 7 and Fig. S10, also in Table S12). We show that the top ten ROGs account for over 50% on ROG emissions, OHR, and OFP (Fig. 7). With the exception of furniture coating industry, the fractions on the top ten species in total emissions, OHR, and OFP from industrial VCP sources were in range of 89%-96%. The lower fractions (ranging from 69% to 86%) of the top ten species in the furniture coating industry may be a result of the wider range of industrial coatings (i.e. both solvent-borne and water-

borne coatings) utilized in this industry. ROGs emitted from industrial VCP sources are apparently more centralized compared to vehicular emissions (ranging from 51% to 87%). Additionally, the cumulative fractions of the top one hundred species in overall ROG emissions, OHR, and OFP in various industrial VCP sources is further indicated the highly centralized of ROG emissions from various emission sources (Fig. S10). More than half of the top ten species in ROG emissions, OHR, and OFP from industrial VCP sources were OVOCs (Table S13). Among them, isopropanol made a notable contribution to the printing, plastic surface coating, and shoemaking industries. Other OVOCs such as MEK, acetone, and ethyl acetate contributed to total ROG emissions in each industry, while formaldehyde, acetaldehyde contributed to total OHR and OFP. It should be noted that the proportions of C_{13}, C_{14}, and C_{15} cycloalkanes from printing industry (account for 6.3% in ROG emissions), as well as the proportion of C_{11} aromatics from ship coating industry (account for 1.0% in ROG emissions) are not negligible. Additionally, acetylacetone is a common species with broad industrial applications, and contributes importantly to secondary pollutants formation under polluted environments (Ji et al., 2018). Although it only contributes 8.7% to total emissions from the furniture coating industry, its fraction in terms of total OHR can be as high as 30%. These findings demonstrated that previously underreported ROGs should receive greater attention in future research.

The updated measurements of OVOC emissions by using the PTR-ToF-MS substantially improve our understanding of the emission of industrial VCP sources. The effective saturation concentrations (C*) of high-molecular-weight OVOCs were found to be lower, which were corresponding to intermediate-volatility organic compounds (IVOCs) and semi-volatile organic compounds (SVOCs). Since these S/I-VOCs are crucial precursors for the SOA in urban environments (Zhao et al., 2014), it is important to comprehend their contributions from the emissions of industrial VCP sources across various volatility classes, including volatility organic compounds (VOCs), IVOCs, and SVOCs (Guenther et al., 2012;Li et al., 2016). Fig. 8 illustrates the distribution of ROG species in a two-dimensional volatility basis set (2D-VBS) space for various industrial

VCP sources, categorized based on volatility bins (Li et al., 2016;Donahue et al., 2011). It is worth noting that the volatility distributions exhibit substantial variation across industrial VCP sources (Fig. 8a). Generally, VOCs constitute the predominant fraction of emissions from industrial VCP sources, accounting for 59% to 98% of the total emissions. The fractions of IVOCs are largest in the printing industry (40%), compared to the range of 2.1%-9.6% in other industrial VCP sources. Conversely, the contribution of SVOCs from industrial VCP sources are negligible in our study, accounting for less than 1%. Considering the importance of S/I-VOCs in SOA formation, particularly with the increasing adoption of improved online mass spectrometry technologies, the S/I-VOCs emissions from industrial VCP sources should be paid more attention in future research.

3.3 Evaluate ROGs treatment efficiency in industrial VCP sources

The analysis of the PTR-ToF-MS mass spectra offers valuable insights into the impact of ROG emissions from industrial VCP sources. This comprehensive information provided by the PTR-ToF-MS also allows for a systematic comparison of emissions before and after the treatment of ROGs. The scatterplot of the concentrations of various ROGs before and after treatment in industrial VCP sources are shown in Fig. 9 and Fig. S11. The observed treatment efficiency, represented by 1-slope, did not reach the desired levels, ranging from -12% to 68%. Among the industrial VCP sources investigated, the shoemaking industry exhibited the highest treatment efficiency (slope=0.32) with the activated carbon adsorption combined with UV photolysis device. This remarkable efficiency can be attributed to the large-scale nature of the factory and meticulous regulation of the ROG treatment devices. Following closely behind is the printing industry, utilizing catalytic combustion devices, with a slightly higher efficacy (slope=0.67) than another treatment device in the same factory (slope=0.80). Nonetheless, it is evident that the treatment efficiency has not reached the desired levels for all ROG groups (Fig. S11), which possibly due to the challenges associated with effectively removing majority ROG emissions using current treatment technologies. Additionally, we also observed that some OVOCs may be generated as byproducts after

the implementation of treatment devices. For instance, the concentrations of CH_2O_2 (e.g. formic acids), $C_4H_6O_3$ (e.g. propylene carbonate), and $C_9H_{18}O$ (e.g. nonanal) were found to be higher after the application of activated carbon adsorption combined with UV photolysis devices (Fig. 9d). Similarly, the concentrations of C_3H_4O (e.g. acrolein) and $C_{12}H_{18}O_4$ (e.g. dibutyl squarate) were also higher following the utilization of catalytic combustion devices (Fig. 9e). Therefore, it is crucial to consider the potential contribution of these ROGs when assessing the emissions released into the atmosphere. The lowest treatment efficiency of ROG was obtained in the furniture coating industry (slope=1.12). This treatment device demonstrates inefficiency for all ROG groups (Fig. S11). The inadequate performance of the ROG treatment devices in this specific facility may be attributed to a number of possible reasons, e.g., delayed replacement of activated carbon and other adsorption materials, and the implementation of the UV photolysis device could potentially result in the generation of more ROGs as byproducts.

Furthermore, the θ angles between the mass spectra of ROG from workshops, before and after ROG treatment devices for various industrial VCP sources were calculated and summarized in Fig. S12 (also in Table. S13). A comparison between the correlation of mass spectra among workshops versus after treatment devices (ranging from 6.2° to 49°) and workshops versus before treatment devices (ranging from 4.2° to 41°) demonstrated a poorer correlation in the former case. The similarities between workshops and stack emissions in the shoemaking industry were lower compared to other industrial VCP sources. This discrepancy can potentially be attributed to the inclusion of ROG emissions from non-VCP usage manufacturing processes (e.g. sole injection molding) in the collection process of ROG treatment devices. Additionally, the θ angles similarity between the mass spectra from before and after ROG treatment devices in various industrial VCP sources also providing insight into the efficacy of the devices in removing ROGs (Fig. 9). The θ angles in ROG treatment devices from five industrial VCP sources were found to range from 1.8° to 27°, indicating good consistency between the mass spectra before and after treatment of ROGs. This alignment suggests that the chemical compositions of ROG emissions remain

comparable before and after treatment ($R \geq 0.87$), implying that the relative proportions of various ROG components are not significantly affected by the ROG treatment devices in these industrial VCP sources.

3.4 Impact of industrial VCP sources on ambient air

To gain deeper insights into the atmospheric impact of emissions from industrial VCP sources, an in-situ measurement was carried out at a monitoring station nearby the furniture coating industry, located 2 km northeast from the industry site. The measurement was conducted using a PTR-ToF-MS (Kore Inc., U.K.), which enabled the quantification of various common ROGs. More information about this instrument and dataset for in-situ measurement can be found elsewhere (Gonzalez-Mendez et al., 2016;Song et al., 2023). Concordant with expectations, the average concentrations of representative ROGs generally demonstrate a discernible decline from the furniture coating industry (including stack emission and workshops during working and non-working hours) to the ambient measurement (Fig. 10). C_8 aromatics and MEK performed considerable emissions from furniture coating industry, while the concentrations of them in the ambient air are orders of magnitude lower than those observed in the industry. However, ambient concentrations of OVOCs, specifically MEK (6.8±8.2 ppb) and ethyl acetate (7.5±5.9 ppb) are still significantly higher than clean environments and are among the highest measured concentration in the literature (Wu et al., 2020a;He et al., 2022b;Khare et al., 2022;Yang et al., 2022). It is confirmed that OVOCs should be paid attention to industrialized urban areas, thereby further substantiating the significance of OVOC emissions from industrial VCP sources to atmospheric pollution. These results stress the invaluable insights provided by PTR-ToF-MS in comprehensively characterizing ROG compositions in both emission sources and urban air.

The preceding discussions illustrate that the emission characteristics of ROGs significantly vary among industrial VCP sources. As a result, the ratio of ROG pairs can be used to distinguish emissions of industrial VCP sources. MEK and C_8 aromatics emerge as key species in industrial VCP emissions, and the reaction rate constants of

C_8 aromatics with OH radical (k_{OH} = (1.4-2.3) × 10^{-11} $cm^3 \cdot molecule^{-1} \cdot s^{-1}$) are higher than MEK ($k_{OH}$ = 5.5 × 10^{-12} $cm^3 \cdot molecule^{-1} \cdot s^{-1}$) (Atkinson and Arey, 2003;Wu et al., 2020a). Fig. 11 illustrates the correlation of MEK with C_8 aromatics in stack emission, workshops during working hours and non-working hours in the furniture coating industry, as well as ambient measurement near the industry. Positive correlations between MEK and C_8 aromatics are observed in both emission sources and ambient measurements, indicating a shared source for these compounds. Additionally, the observed ratios of MEK to C_8 aromatics in ambient measurement are also comparable with the ratios of MEK to C_8 aromatics measured in emissions from the furniture coating industry (0.97 $ppb \cdot ppb^{-1}$ for the stack emission and 0.75 $ppb \cdot ppb^{-1}$ for the workshops emission), suggesting that industrial VCP emissions (specifically furniture coating) may account for the enhancement of MEK and C_8 aromatics in this industrial area. The peak concentration of MEK exceeding 200 ppb from the ambient measurements are among the highest in the literature (Fig. 11). Therefore, we conducted a comparison of MEK and C_8 aromatics concentrations in this study with those in clean environments (urban, rural, forest, and coastal sites) from previous studies (Fig. S13) (Wu et al., 2020a;Coggon et al., 2024;Yuan et al., 2012;Seco et al., 2011;Acton et al., 2016;Tan et al., 2021;He et al., 2022b). It is indicating that ambient measurements in industrial areas have been significantly impacted by industrial VCP sources, and the MEK / C_8 aromatics ratio can serve as good evidence by using high time-resolution ROG measurements from PTR-ToF-MS.

4. Conclusion

In this work, we conducted a field campaign to measure more comprehensive speciation of ROG emissions from industrial VCP sources, including shoemaking, plastic surface coating, furniture coating, printing, and ship coating industries. To achieve this, we employed the PTR-ToF-MS in combination with canister-GC-MS/FID techniques. Our study demonstrated that OVOCs have been identified as representative ROGs emitted from these sources, which are highly related to specific chemicals used during the industrial activities. Furthermore, we performed a mass spectra similarity

analysis to compare the ROG emissions across different emission sources. The poor consistency of the similarity between the mass spectra in emission sources indicating that substantial differences between industrial VCP sources, as they cannot be directly categorized as a single class of emission sources.

In addition, the fractions of ROGs in total ROG emissions and OHR are determined by combining measurements from canister-GC-MS/FID and PTR-ToF-MS. Except for the ship coating industry utilizing solvent-borne coatings, the proportions of OVOCs range from 67% to 96% in total ROG emissions and 72% to 97% in total OHR for different industrial sources. Large fraction of OVOCs may be related to two reasons: (1) more OVOC species are detected in this study; (2) water-borne coatings and inks are more widely employed in the recent year which may enhance OVOC fractions. This highlights the importance of measuring these OVOC emissions from industrial VCP sources. The industrial VCP sources associated with solvent-borne coatings exhibited a higher OFP, reaching as high as 5.5 and 2.7 g $O_3 \cdot g^{-1}$ ROGs for ship coating and furniture coating industries, primarily due to contributions from aromatics, suggesting that these sources should be controlled in priority. The fractions of the ten most abundant species in total ROG emissions, OHR, and OFP indicate the highly centralized of ROG emissions from various emission sources.

Our results suggest that ROG treatment devices may have limited effectiveness in removing ROGs, with treatment efficiencies ranging from -12% to 68%. In addition, OVOCs should be paid more attention to industrialized urban areas due to the substantial impact of industrial VCP sources. Our study demonstrated that ROG pairs (e.g., MEK / C_8 aromatics ratio) can be utilized as reliable evidence for indicating the impact of industrial VCP sources on ambient measurements in industrial areas.

This study highlights the significant role of OVOCs to ROG emissions from industrial VCP sources, particularly those utilizing water-borne chemicals. As a result, these industrial VCP sources may significantly contribute to the primary emissions of OVOCs in urban regions. The current emission inventories do not fully account for the emissions of many ROGs, which can compromise the predictive accuracy of air quality

models in urban areas. In this study, a broader range of ROG species was quantified using PTR-ToF-MS measurements, which highlights the effectiveness of PTR-ToF-MS in characterizing ROG emissions from industrial VCP sources.

Data availability

Data are available from the authors upon request.

Author contribution

BY designed the research. BY and SHW organized industrial VCP source measurements. SHW, XJH, RC, CHW, and CMW contributed to data collection. SHW performed the data analysis, with contributions from XS and YBC. SHW and BY prepared the manuscript with contributions from YBH, XBL, BGW and MS. All the authors reviewed the manuscript.

Competing interests

The authors declare that they have no known competing financial interests or personal relationships that could have appeared to influence the work reported in this paper.

Acknowledgement

This work was supported by the National Key R&D Plan of China (grant No. 2022YFC3700604), the National Natural Science Foundation of China (grant No. 42230701, and 42205094). This work was also Supported by the Outstanding Innovative Talents Cultivation Funded Programs for Doctoral Students of Jinan University (grant No.2022CXB028).

References

Acton, W. J. F., Schallhart, S., Langford, B., Valach, A., Rantala, P., Fares, S., Carriero, G., Tillmann, R., Tomlinson, S. J., Dragosits, U., Gianelle, D., Hewitt, C. N., and Nemitz, E.: Canopy-scale flux measurements and bottom-up emission estimates of volatile organic compounds from a mixed oak and hornbeam forest in northern Italy, Atmospheric Chemistry and Physics, 16, 7149-7170, 10.5194/acp-16-7149-2016, 2016.

Atkinson, R., and Arey, J.: Atmospheric Degradation of Volatile Organic Compounds, Chemical Reviews, 103, 4605-4638, 10.1021/cr0206420, 2003.

Atkinson, R., Baulch, D. L., Cox, R. A., Crowley, J. N., Hampson, R. F., Hynes, R. G., Jenkin, M. E., Rossi, M. J., and Troe, J.: Evaluated kinetic and photochemical data for atmospheric chemistry: Volume I - gas phase reactions of Ox, HOx, NOx and SOx species, Atmos. Chem. Phys., 4, 1461-1738, 10.5194/acp-4-1461-2004, 2004.

Atkinson, R., Baulch, D. L., Cox, R. A., Crowley, J. N., Hampson, R. F., Hynes, R. G., Jenkin, M. E., Rossi, M. J., Troe, J., and Subcommittee, I.: Evaluated kinetic and photochemical data for atmospheric chemistry: Volume II – gas phase reactions of organic species, Atmos. Chem. Phys., 6, 3625-4055, 10.5194/acp-6-3625-2006, 2006.

Buhr, K., van Ruth, S., and Delahunty, C.: Analysis of volatile flavour compounds by Proton Transfer Reaction-Mass Spectrometry: fragmentation patterns and discrimination between isobaric and isomeric compounds, International Journal of Mass Spectrometry, 221, 1-7, https://doi.org/10.1016/S1387-3806(02)00896-5, 2002.

Cappellin, L., Karl, T., Probst, M., Ismailova, O., Winkler, P. M., Soukoulis, C., Aprea, E., Mark, T. D., Gasperi, F., and Biasioli, F.: On quantitative determination of volatile organic compound concentrations using proton transfer reaction time-of-flight mass spectrometry, Environmental Science & Technology, 46, 2283-2290, 10.1021/es203985t, 2012.

Carter, W. P.: Development of the SAPRC-07 chemical mechanism and updated ozone reactivity scales, Citeseer, 2007.

Chang, X., Zhao, B., Zheng, H., Wang, S., Cai, S., Guo, F., Gui, P., Huang, G., Wu, D., Han, L., Xing, J., Man, H., Hu, R., Liang, C., Xu, Q., Qiu, X., Ding, D., Liu, K., Han, R., Robinson, A. L., and Donahue, N. M.: Full-volatility emission framework corrects missing and underestimated secondary organic aerosol sources, One Earth, 5, 403-412, https://doi.org/10.1016/j.oneear.2022.03.015, 2022.

Chen, Y., Yuan, B., Wang, C., Wang, S., He, X., Wu, C., Song, X., Huangfu, Y., Li, X. B., Liao, Y., and Shao, M.: Online measurements of cycloalkanes based on NO^+ chemical ionization in proton transfer reaction time-of-flight mass spectrometry (PTR-ToF-MS), Atmos. Meas. Tech., 15, 6935-6947, 10.5194/amt-15-6935-2022, 2022.

Coggon, M. M., McDonald, B. C., Vlasenko, A., Veres, P. R., Bernard, F., Koss, A. R., Yuan, B., Gilman, J. B., Peischl, J., Aikin, K. C., DuRant, J., Warneke, C., Li, S. M., and de Gouw, J. A.: Diurnal Variability and Emission Pattern of Decamethylcyclopentasiloxane (D5) from the Application of Personal Care Products in Two North American Cities, Environ Sci Technol, 52, 5610-5618, 10.1021/acs.est.8b00506, 2018.

Coggon, M. M., Gkatzelis, G. I., McDonald, B. C., Gilman, J. B., Schwantes, R. H., Abuhassan, N., Aikin, K. C., Arend, M. F., Berkoff, T. A., Brown, S. S., Campos, T. L., Dickerson, R. R., Gronoff, G., Hurley, J. F., Isaacman-VanWertz, G., Koss, A. R., Li, M., McKeen, S. A., Moshary, F., Peischl, J., Pospisilova, V., Ren, X., Wilson, A., Wu, Y., Trainer, M., and Warneke, C.: Volatile chemical product emissions enhance ozone and modulate urban chemistry, Proc Natl Acad Sci U S A, 118, 10.1073/pnas.2026653118, 2021.

Coggon, M. M., Stockwell, C. E., Claflin, M. S., Pfannerstill, E. Y., Xu, L., Gilman, J. B., Marcantonio, J., Cao, C., Bates, K., Gkatzelis, G. I., Lamplugh, A., Katz, E. F., Arata, C., Apel, E. C., Hornbrook, R. S., Piel, F., Majluf, F., Blake, D. R., Wisthaler, A., Canagaratna, M., Lerner, B. M., Goldstein, A. H., Mak, J. E., and Warneke, C.: Identifying and correcting interferences to PTR-ToF-MS measurements of isoprene and other urban volatile organic compounds, Atmospheric Measurement Techniques, 17, 801-825, 10.5194/amt-17-801-2024, 2024.

de Gouw, J., and Warneke, C.: Measurements of volatile organic compounds in the earth's atmosphere using proton-transfer-reaction mass spectrometry, Mass Spectrom Rev 26, 223-257, 10.1002/mas.20119, 2007.

Donahue, N. M., Epstein, S. A., Pandis, S. N., and Robinson, A. L.: A two-dimensional volatility basis set: 1. organic-aerosol mixing thermodynamics, Atmospheric Chemistry and Physics, 11, 3303-3318, 10.5194/acp-11-3303-2011, 2011.

Fang, L., Liu, W., Chen, D., Li, G., Wang, D., Shao, X., and Nie, L.: Source Profiles of Volatile Organic Compounds (VOCs) from Typical Solventbased Industries in Beijing (in Chinese), Environmental Science, 40, 4395-4403, 10.13227/j.hjkx.201901128, 2019.

Fortner, E. C., Zheng, J., Zhang, R., Berk Knighton, W., Volkamer, R. M., Sheehy, P., Molina, L., and André, M.: Measurements of Volatile Organic Compounds Using Proton Transfer Reaction – Mass Spectrometry during the MILAGRO 2006 Campaign, Atmos. Chem. Phys., 9, 467-481, 10.5194/acp-9-467-2009, 2009.

Gao, Y., Wang, H., Yuan, L., Jing, S., Yuan, B., Shen, G., Zhu, L., Koss, A., Li, Y., Wang, Q., Huang, D. D., Zhu, S., Tao, S., Lou, S., and Huang, C.: Measurement report: Underestimated reactive organic gases from residential combustion – insights from a near-complete speciation, Atmospheric Chemistry and Physics, 23, 6633-6646, 10.5194/acp-23-6633-2023, 2023.

Gkatzelis, G. I., Coggon, M. M., McDonald, B. C., Peischl, J., Aikin, K. C., Gilman, J. B., Trainer, M., and Warneke, C.: Identifying Volatile Chemical Product Tracer Compounds in U.S. Cities, Environ Sci Technol, 55, 188-199, 10.1021/acs.est.0c05467, 2021a.

Gkatzelis, G. I., Coggon, M. M., McDonald, B. C., Peischl, J., Gilman, J. B., Aikin, K. C., Robinson, M. A., Canonaco, F., Prevot, A. S. H., Trainer, M., and Warneke, C.: Observations Confirm that Volatile Chemical Products Are a Major Source of Petrochemical Emissions in U.S. Cities, Environ Sci Technol, 55, 4332-4343, 10.1021/acs.est.0c05471, 2021b.

Gonzalez-Mendez, R., Watts, P., Olivenza-Leon, D., Reich, D. F., Mullock, S. J., Corlett, C. A., Cairns, S., Hickey, P., Brookes, M., and Mayhew, C. A.: Enhancement of

Compound Selectivity Using a Radio Frequency Ion-Funnel Proton Transfer Reaction Mass Spectrometer: Improved Specificity for Explosive Compounds, Anal Chem, 88, 10624-10630, 10.1021/acs.analchem.6b02982, 2016.
Guenther, A. B., Jiang, X., Heald, C. L., Sakulyanontvittaya, T., Duhl, T., Emmons, L. K., and Wang, X.: The Model of Emissions of Gases and Aerosols from Nature version 2.1 (MEGAN2.1): an extended and updated framework for modeling biogenic emissions, Geoscientific Model Development, 5, 1471-1492, 10.5194/gmd-5-1471-2012, 2012.
Haase, K. B., Keene, W. C., Pszenny, A. A. P., Mayne, H. R., Talbot, R. W., and Sive, B. C.: Calibration and intercomparison of acetic acid measurements using proton-transfer-reaction mass spectrometry (PTR-MS), Atmospheric Measurement Techniques, 5, 2739-2750, 10.5194/amt-5-2739-2012, 2012.
Han, C., Liu, R., Luo, H., Li, G., Ma, S., Chen, J., and An, T.: Pollution profiles of volatile organic compounds from different urban functional areas in Guangzhou China based on GC/MS and PTR-TOF-MS: Atmospheric environmental implications, Atmospheric Environment, 214, 10.1016/j.atmosenv.2019.116843, 2019.
He, X., Che, X., Gao, S., Chen, X., Pan, M., Jiang, M., Zhang, S., Jia, H., and Duan, Y.: Volatile organic compounds emission inventory of organic chemical raw material industry, Atmospheric Pollution Research, 13, 10.1016/j.apr.2021.101276, 2022a.
He, X., Yuan, B., Wu, C., Wang, S., Wang, C., Huangfu, Y., Qi, J., Ma, N., Xu, W., Wang, M., Chen, W., Su, H., Cheng, Y., and Shao, M.: Volatile organic compounds in wintertime North China Plain: Insights from measurements of proton transfer reaction time-of-flight mass spectrometer (PTR-ToF-MS), Journal of Environmental Sciences, 10.1016/j.jes.2021.08.010, 2022b.
Huang, C., Chen, C. H., Li, L., Cheng, Z., Wang, H. L., Huang, H. Y., Streets, D. G., Wang, Y. J., Zhang, G. F., and Chen, Y. R.: Emission inventory of anthropogenic air pollutants and VOC species in the Yangtze River Delta region, China, Atmospheric Chemistry and Physics, 11, 4105-4120, 10.5194/acp-11-4105-2011, 2011.
Huangfu, Y., Yuan, B., Wang, S., Wu, C., He, X., Qi, J., de Gouw, J., Warneke, C., Gilman, J. B., Wisthaler, A., Karl, T., Graus, M., Jobson, B. T., and Shao, M.: Revisiting Acetonitrile as Tracer of Biomass Burning in Anthropogenic-Influenced Environments, Geophysical Research Letters, 48, 10.1029/2020gl092322, 2021.
Humes, M. B., Wang, M., Kim, S., Machesky, J. E., Gentner, D. R., Robinson, A. L., Donahue, N. M., and Presto, A. A.: Limited Secondary Organic Aerosol Production from Acyclic Oxygenated Volatile Chemical Products, Environ Sci Technol, 56, 4806-4815, 10.1021/acs.est.1c07354, 2022.
Inomata, S., Tanimoto, H., and Yamada, H.: Mass Spectrometric Detection of Alkanes Using NO+ Chemical Ionization in Proton-transfer-reaction Plus Switchable Reagent Ion Mass Spectrometry, Chemistry Letters, 43, 538-540, 10.1246/cl.131105, 2014.
Ji, Y., Zheng, J., Qin, D., Li, Y., Gao, Y., Yao, M., Chen, X., Li, G., An, T., and Zhang, R.: OH-Initiated Oxidation of Acetylacetone: Implications for Ozone and Secondary Organic Aerosol Formation, Environ Sci Technol, 52, 11169-11177, 10.1021/acs.est.8b03972, 2018.

Kamal, M. S., Razzak, S. A., and Hossain, M. M.: Catalytic oxidation of volatile organic compounds (VOCs) – A review, Atmospheric Environment, 140, 117-134, 10.1016/j.atmosenv.2016.05.031, 2016.
Khare, P., and Gentner, D. R.: Considering the future of anthropogenic gas-phase organic compound emissions and the increasing influence of non-combustion sources on urban air quality, Atmospheric Chemistry and Physics, 18, 5391-5413, 10.5194/acp-18-5391-2018, 2018.
Khare, P., Krechmer, J. E., Machesky, J. E., Hass-Mitchell, T., Cao, C., Wang, J., Majluf, F., Lopez-Hilfiker, F., Malek, S., Wang, W., Seltzer, K., Pye, H. O. T., Commane, R., McDonald, B. C., Toledo-Crow, R., Mak, J. E., and Gentner, D. R.: Ammonium adduct chemical ionization to investigate anthropogenic oxygenated gas-phase organic compounds in urban air, Atmospheric Chemistry and Physics, 22, 14377-14399, 10.5194/acp-22-14377-2022, 2022.
Koss, A. R., Warneke, C., Yuan, B., Coggon, M. M., Veres, P. R., and de Gouw, J. A.: Evaluation of NO^+ reagent ion chemistry for online measurements of atmospheric volatile organic compounds, Atmospheric Measurement Techniques, 9, 2909-2925, 10.5194/amt-9-2909-2016, 2016.
Koss, A. R., Sekimoto, K., Gilman, J. B., Selimovic, V., Coggon, M. M., Zarzana, K. J., Yuan, B., Lerner, B. M., Brown, S. S., Jimenez, J. L., Krechmer, J., Roberts, J. M., Warneke, C., Yokelson, R. J., and de Gouw, J.: Non-methane organic gas emissions from biomass burning: identification, quantification, and emission factors from PTR-ToF during the FIREX 2016 laboratory experiment, Atmospheric Chemistry and Physics, 18, 3299-3319, 10.5194/acp-18-3299-2018, 2018.
Kostenidou, E., Lee, B.-H., Engelhart, G. J., Pierce, J. R., and Pandis, S. N.: Mass Spectra Deconvolution of Low, Medium, and High Volatility Biogenic Secondary Organic Aerosol, Environmental Science & Technology, 43, 4884-4889, 10.1021/es803676g, 2009.
Li, C., Cui, M., Zheng, J., Chen, Y., Liu, J., Ou, J., Tang, M., Sha, Q., Yu, F., Liao, S., Zhu, M., Wang, J., Yao, N., and Li, C.: Variability in real-world emissions and fuel consumption by diesel construction vehicles and policy implications, Sci Total Environ, 786, 147256, 10.1016/j.scitotenv.2021.147256, 2021.
Li, G., Jiang, B., Wang, S., Li, C., Yuan, B., Wang, B., and Zhanyi, Z.: Determination of 118 Volatile Organic Compounds in Source Emission by Canister Sampling-Preconcentration /Gas Chromatography − Mass Spectrometry (in Chinese), Journal of Instrumental Analysis, 39, 1441-1450, 2020.
Li, L., and Cocker, D. R.: Molecular structure impacts on secondary organic aerosol formation from glycol ethers, Atmospheric Environment, 180, 206-215, 10.1016/j.atmosenv.2017.12.025, 2018.
Li, M., Zhang, Q., Zheng, B., Tong, D., Lei, Y., Liu, F., Hong, C. P., Kang, S. C., Yan, L., Zhang, Y. X., Bo, Y., Su, H., Cheng, Y. F., and He, K. B.: Persistent growth of anthropogenic non-methane volatile organic compound (NMVOC) emissions in China during 1990–2017: drivers, speciation and ozone formation potential, Atmospheric Chemistry and Physics, 19, 8897-8913, 10.5194/acp-19-8897-2019, 2019.

Li, W., Li, L., Chen, C.-l., Kacarab, M., Peng, W., Price, D., Xu, J., and Cocker, D. R.: Potential of select intermediate-volatility organic compounds and consumer products for secondary organic aerosol and ozone formation under relevant urban conditions, Atmospheric Environment, 178, 109-117, 10.1016/j.atmosenv.2017.12.019, 2018.

Li, X.-B., Yuan, B., Wang, S., Wang, C., Lan, J., Liu, Z., Song, Y., He, X., Huangfu, Y., Pei, C., Cheng, P., Yang, S., Qi, J., Wu, C., Huang, S., You, Y., Chang, M., Zheng, H., Yang, W., Wang, X., and Shao, M.: Variations and sources of volatile organic compounds (VOCs) in urban region: insights from measurements on a tall tower, Atmospheric Chemistry and Physics, 22, 10567-10587, 10.5194/acp-22-10567-2022, 2022.

Li, X.-B., Zhang, C., Liu, A., Yuan, B., Yang, H., Liu, C., Wang, S., Huangfu, Y., Qi, J., Liu, Z., He, X., Song, X., Chen, Y., Peng, Y., Zhang, X., Zheng, E., Yang, L., Yang, Q., Qin, G., Zhou, J., and Shao, M.: Assessment of long tubing in measuring atmospheric trace gases: applications on tall towers, Environmental Science: Atmospheres, 10.1039/d2ea00110a, 2023.

Li, Y., Pöschl, U., and Shiraiwa, M.: Molecular corridors and parameterizations of volatility in the chemical evolution of organic aerosols, Atmospheric Chemistry and Physics, 16, 3327-3344, 10.5194/acp-16-3327-2016, 2016.

Liang, Z., Chen, L., Alam, M. S., Zeraati Rezaei, S., Stark, C., Xu, H., and Harrison, R. M.: Comprehensive chemical characterization of lubricating oils used in modern vehicular engines utilizing GC × GC-TOFMS, Fuel, 220, 792-799, 10.1016/j.fuel.2017.11.142, 2018.

Liu, Y., Li, Y., Yuan, Z., Wang, H., Sha, Q., Lou, S., Liu, Y., Hao, Y., Duan, L., Ye, P., Zheng, J., Yuan, B., and Shao, M.: Identification of two main origins of intermediate-volatility organic compound emissions from vehicles in China through two-phase simultaneous characterization, Environ Pollut, 281, 117020, 10.1016/j.envpol.2021.117020, 2021.

Malherbe, L., and Mandin, C.: VOC emissions during outdoor ship painting and health-risk assessment, Atmospheric Environment, 41, 6322-6330, 10.1016/j.atmosenv.2007.02.018, 2007.

McDonald, B. C., de Gouw, J. A., Gilman, J. B., Jathar, S. H., Akherati, A., Cappa, C. D., Jimenez, J. L., Lee-Taylor, J., Hayes, P. L., McKeen, S. A., Cui, Y. Y., Kim, S.-W., Gentner, D. R., Isaacman-VanWertz, G., Goldstein, A. H., Harley, R. A., Frost, G. J., Roberts, J. M., Ryerson, T. B., and Trainer, M.: Volatile chemical products emerging as largest petrochemical source of urban organic emissions, Science, 359, 760, 10.1126/science.aaq0524, 2018.

Mo, Z., Shao, M., and Lu, S.: Compilation of a source profile database for hydrocarbon and OVOC emissions in China, Atmospheric Environment, 143, 209-217, 10.1016/j.atmosenv.2016.08.025, 2016.

Mo, Z., Cui, R., Yuan, B., Cai, H., McDonald, B. C., Li, M., Zheng, J., and Shao, M.: A mass-balance-based emission inventory of non-methane volatile organic compounds (NMVOCs) for solvent use in China, Atmospheric Chemistry and Physics, 21, 13655-13666, 10.5194/acp-21-13655-2021, 2021.

Na, K., and Pyo Kim, Y.: Chemical mass balance receptor model applied to ambient C_2–C_9 VOC concentration in Seoul, Korea: Effect of chemical reaction losses, Atmospheric Environment, 41, 6715-6728, https://doi.org/10.1016/j.atmosenv.2007.04.054, 2007.
Ou, J., Zheng, J., Li, R., Huang, X., Zhong, Z., Zhong, L., and Lin, H.: Speciated OVOC and VOC emission inventories and their implications for reactivity-based ozone control strategy in the Pearl River Delta region, China, Sci Total Environ, 530-531, 393-402, 10.1016/j.scitotenv.2015.05.062, 2015.
Qin, M., Murphy, B. N., Isaacs, K. K., McDonald, B. C., Lu, Q., McKeen, S. A., Koval, L., Robinson, A. L., Efstathiou, C., Allen, C., and Pye, H. O. T.: Criteria pollutant impacts of volatile chemical products informed by near-field modelling, Nature Sustainability, 4, 129-137, 10.1038/s41893-020-00614-1, 2021.
Rogers, T. M., Grimsrud, E. P., Herndon, S. C., Jayne, J. T., Kolb, C. E., Allwine, E., Westberg, H., Lamb, B. K., Zavala, M., Molina, L. T., Molina, M. J., and Knighton, W. B.: On-road measurements of volatile organic compounds in the Mexico City metropolitan area using proton transfer reaction mass spectrometry, International Journal of Mass Spectrometry, 252, 26-37, 10.1016/j.ijms.2006.01.027, 2006.
Sasidharan, S., He, Y., Akherati, A., Li, Q., Li, W., Cocker, D., McDonald, B. C., Coggon, M. M., Seltzer, K. M., Pye, H. O. T., Pierce, J. R., and Jathar, S. H.: Secondary Organic Aerosol Formation from Volatile Chemical Product Emissions: Model Parameters and Contributions to Anthropogenic Aerosol, Environmental Science & Technology, 57, 11891-11902, 10.1021/acs.est.3c00683, 2023.
Seco, R., Peñuelas, J., Filella, I., Llusià, J., Molowny-Horas, R., Schallhart, S., Metzger, A., Müller, M., and Hansel, A.: Contrasting winter and summer VOC mixing ratios at a forest site in the Western Mediterranean Basin: the effect of local biogenic emissions, Atmospheric Chemistry and Physics, 11, 13161-13179, 10.5194/acp-11-13161-2011, 2011.
Sekimoto, K., Li, S.-M., Yuan, B., Koss, A., Coggon, M., Warneke, C., and de Gouw, J.: Calculation of the sensitivity of proton-transfer-reaction mass spectrometry (PTR-MS) for organic trace gases using molecular properties, International Journal of Mass Spectrometry, 421, 71-94, 10.1016/j.ijms.2017.04.006, 2017.
Seltzer, K. M., Pennington, E., Rao, V., Murphy, B. N., Strum, M., Isaacs, K. K., and Pye, H. O. T.: Reactive organic carbon emissions from volatile chemical products, Atmos Chem Phys, 21, 5079-5100, 10.5194/acp-21-5079-2021, 2021.
Seltzer, K. M., Murphy, B. N., Pennington, E. A., Allen, C., Talgo, K., and Pye, H. O. T.: Volatile Chemical Product Enhancements to Criteria Pollutants in the United States, Environ Sci Technol, 56, 6905-6913, 10.1021/acs.est.1c04298, 2022.
Sha, Q., Zhu, M., Huang, H., Wang, Y., Huang, Z., Zhang, X., Tang, M., Lu, M., Chen, C., Shi, B., Chen, Z., Wu, L., Zhong, Z., Li, C., Xu, Y., Yu, F., Jia, G., Liao, S., Cui, X., Liu, J., and Zheng, J.: A newly integrated dataset of volatile organic compounds (VOCs) source profiles and implications for the future development of VOCs profiles in China, Sci Total Environ, 793, 148348, 10.1016/j.scitotenv.2021.148348, 2021.
Shi, Y., Xi, Z., Lv, D., Simayi, M., Liang, Y., Ren, J., and Xie, S.: Sector-based volatile organic compound emission characteristics and reduction perspectives for coating

materials manufacturing in China, Journal of Cleaner Production, 394, 10.1016/j.jclepro.2023.136407, 2023.
Song, X., Yuan, B., Wang, S., He, X., Li, X., Peng, Y., Chen, Y., Qi, J., Cai, J., Huang, s., Hu, D., Wei, W., Liu, K., and Shao, M.: Compositional Characteristics of Volatile Organic Compounds in Typical Industrial Areas of the Pearl River Delta: Importance of Oxygenated Volatile Organic Compounds (in Chinese), Environmental Science, 10.13227/j.hjkx.202204104, 2023.
Stark, H., Yatavelli, R. L. N., Thompson, S. L., Kimmel, J. R., Cubison, M. J., Chhabra, P. S., Canagaratna, M. R., Jayne, J. T., Worsnop, D. R., and Jimenez, J. L.: Methods to extract molecular and bulk chemical information from series of complex mass spectra with limited mass resolution, International Journal of Mass Spectrometry, 389, 26-38, 10.1016/j.ijms.2015.08.011, 2015.
Stockwell, C. E., Coggon, M. M., Gkatzelis, G. I., Ortega, J., McDonald, B. C., Peischl, J., Aikin, K., Gilman, J. B., Trainer, M., and Warneke, C.: Volatile organic compound emissions from solvent- and water-borne coatings – compositional differences and tracer compound identifications, Atmospheric Chemistry and Physics, 21, 6005-6022, 10.5194/acp-21-6005-2021, 2021.
Sulzer, P., Hartungen, E., Hanel, G., Feil, S., Winkler, K., Mutschlechner, P., Haidacher, S., Schottkowsky, R., Gunsch, D., Seehauser, H., Striednig, M., Jürschik, S., Breiev, K., Lanza, M., Herbig, J., Märk, L., Märk, T. D., and Jordan, A.: A Proton Transfer Reaction-Quadrupole interface Time-Of-Flight Mass Spectrometer (PTR-QiTOF): High speed due to extreme sensitivity, International Journal of Mass Spectrometry, 368, 1-5, 10.1016/j.ijms.2014.05.004, 2014.
Sun, W., Shao, M., Granier, C., Liu, Y., Ye, C. S., and Zheng, J. Y.: Long-Term Trends of Anthropogenic SO_2, NOx, CO, and NMVOCs Emissions in China, Earth's Future, 6, 1112-1133, 10.1029/2018ef000822, 2018.
Tan, Y., Han, S., Chen, Y., Zhang, Z., Li, H., Li, W., Yuan, Q., Li, X., Wang, T., and Lee, S.-c.: Characteristics and source apportionment of volatile organic compounds (VOCs) at a coastal site in Hong Kong, Science of The Total Environment, 777, 10.1016/j.scitotenv.2021.146241, 2021.
Ulbrich, I. M., Canagaratna, M. R., Zhang, Q., Worsnop, D. R., and Jimenez, J. L.: Interpretation of organic components from Positive Matrix Factorization of aerosol mass spectrometric data, Atmos. Chem. Phys., 9, 2891-2918, 10.5194/acp-9-2891-2009, 2009.
Wang, C., Yuan, B., Wu, C., Wang, S., Qi, J., Wang, B., Wang, Z., Hu, W., Chen, W., Ye, C., Wang, W., Sun, Y., Wang, C., Huang, S., Song, W., Wang, X., Yang, S., Zhang, S., Xu, W., Ma, N., Zhang, Z., Jiang, B., Su, H., Cheng, Y., Wang, X., and Shao, M.: Measurements of higher alkanes using NO^+ chemical ionization in PTR-ToF-MS: important contributions of higher alkanes to secondary organic aerosols in China, Atmospheric Chemistry and Physics, 20, 14123-14138, 10.5194/acp-20-14123-2020, 2020.
Wang, H., Qiao, Y., Chen, C., Lu, J., Dai, H., Qiao, L., Lou, S., Huang, C., Li, L., Jing, S., and Wu, J.: Source Profiles and Chemical Reactivity of Volatile Organic Compounds

from Solvent Use in Shanghai, China, Aerosol and Air Quality Research, 14, 301-310, 10.4209/aaqr.2013.03.0064, 2014.
Wang, H., Sun, S., Nie, L., Zhang, Z., Li, W., and Hao, Z.: A review of whole-process control of industrial volatile organic compounds in China, Journal of Environmental Sciences, 123, 127-139, 10.1016/j.jes.2022.02.037, 2023.
Wang, R., Zhang, C., Ding, H., LV, S., Ding, Y., Wang, H., and Wang, B.: Emission characteristics of volatile organic compounds (VOCs) from the production processes of plastic parts in electronic manufacturing industry (in Chinese), Acta Scientiae Circumstantiae, 39, 4-12, 10.13671/j.hjkxxb.2018.0243, 2019.
Wang, S., Yuan, B., Wu, C., Wang, C., Li, T., He, X., Huangfu, Y., Qi, J., Li, X. B., Sha, Q., Zhu, M., Lou, S., Wang, H., Karl, T., Graus, M., Yuan, Z., and Shao, M.: Oxygenated volatile organic compounds (VOCs) as significant but varied contributors to VOC emissions from vehicles, Atmos. Chem. Phys., 22, 9703-9720, 10.5194/acp-22-9703-2022, 2022.
Wei, W., Wang, S., Hao, J., and Cheng, S.: Projection of anthropogenic volatile organic compounds (VOCs) emissions in China for the period 2010–2020, Atmospheric Environment, 45, 6863-6871, https://doi.org/10.1016/j.atmosenv.2011.01.013, 2011.
Wu, C., Wang, C., Wang, S., Wang, W., Yuan, B., Qi, J., Wang, B., Wang, H., Wang, C., Song, W., Wang, X., Hu, W., Lou, S., Ye, C., Peng, Y., Wang, Z., Huangfu, Y., Xie, Y., Zhu, M., Zheng, J., Wang, X., Jiang, B., Zhang, Z., and Shao, M.: Measurement report: Important contributions of oxygenated compounds to emissions and chemistry of volatile organic compounds in urban air, Atmospheric Chemistry and Physics, 20, 14769-14785, 10.5194/acp-20-14769-2020, 2020a.
Wu, J., Gao, S., Chen, X., Yang, Y., Fu, Q.-y., Che, X., and Jiao, Z.: Source Profiles and Impact of Volatile Organic Compounds in the Coating Manufacturing Industry (in Chinese), Environmental Science, 41, 1582-1588, 10.13227/j.hjkx.201908203, 2020b.
Yang, G., Huo, J., Wang, L., Wang, Y., Wu, S., Yao, L., Fu, Q., and Wang, L.: Total OH Reactivity Measurements in a Suburban Site of Shanghai, Journal of Geophysical Research: Atmospheres, 127, 10.1029/2021jd035981, 2022.
Yang, Y., Shao, M., Wang, X., Nölscher, A. C., Kessel, S., Guenther, A., and Williams, J.: Towards a quantitative understanding of total OH reactivity: A review, Atmospheric Environment, 134, 147-161, https://doi.org/10.1016/j.atmosenv.2016.03.010, 2016.
Yuan, B., Shao, M., Lu, S., and Wang, B.: Source profiles of volatile organic compounds associated with solvent use in Beijing, China, Atmospheric Environment, 44, 1919-1926, 10.1016/j.atmosenv.2010.02.014, 2010.
Yuan, B., Shao, M., Gouw, J. D., Parrish, D. D., Lu, S., Wang, M., Zeng, L., Zhang, Q., Song, Y., and Zhang, J.: Volatile organic compounds (VOCs) in urban air: How chemistry affects the interpretation of positive matrix factorization (PMF) analysis, Journal of Geophysical Research Atmospheres, 117, 24302, 2012.
Yuan, B., Koss, A. R., Warneke, C., Coggon, M., Sekimoto, K., and de Gouw, J. A.: Proton-Transfer-Reaction Mass Spectrometry: Applications in Atmospheric Sciences, Chemical Reviews, 117, 13187-13229, 10.1021/acs.chemrev.7b00325, 2017.
Zhao, J., Yao, X., Sun, M., Xu, Y., Wang, S., Cao, D., and Liu, J.: Emission characteristics of volatile organic compounds from typical solvent use industries in

Tianjin (in Chinese), Environmental Pollution & Control, 43, 539-545, 10.15985/j.cnki.1001-3865.2021.05.002, 2021.
Zhao, R., Huang, L., Zhang, J., and Ouyang, F.: Emissions characteristics of volatile organic compounds (VOCs) from typical industries of solvent use in Chengdu City (in Chinese), Acta Scientiae Circumstantiae, 38, 1147-1154, 10.13671 /j.hjkxxb.2017.0362, 2018a.
Zhao, Y., Hennigan, C. J., May, A. A., Tkacik, D. S., de Gouw, J. A., Gilman, J. B., Kuster, W. C., Borbon, A., and Robinson, A. L.: Intermediate-volatility organic compounds: a large source of secondary organic aerosol, Environ Sci Technol, 48, 13743-13750, 10.1021/es5035188, 2014.
Zhao, Y., Nguyen, N. T., Presto, A. A., Hennigan, C. J., May, A. A., and Robinson, A. L.: Intermediate Volatility Organic Compound Emissions from On-Road Gasoline Vehicles and Small Off-Road Gasoline Engines, Environmental Science & Technology, 50, 4554-4563, 10.1021/acs.est.5b06247, 2016.
Zhao, Y., Lambe, A. T., Saleh, R., Saliba, G., and Robinson, A. L.: Secondary Organic Aerosol Production from Gasoline Vehicle Exhaust: Effects of Engine Technology, Cold Start, and Emission Certification Standard, Environ Sci Technol, 52, 1253-1261, 10.1021/acs.est.7b05045, 2018b.
Zheng, J., Yu, Y., Mo, Z., Zhang, Z., Wang, X., Yin, S., Peng, K., Yang, Y., Feng, X., and Cai, H.: Industrial sector-based volatile organic compound (VOC) source profiles measured in manufacturing facilities in the Pearl River Delta, China, Sci Total Environ, 456-457, 127-136, 10.1016/j.scitotenv.2013.03.055, 2013.
Zhong, Z., Sha, Q., Zheng, J., Yuan, Z., Gao, Z., Ou, J., Zheng, Z., Li, C., and Huang, Z.: Sector-based VOCs emission factors and source profiles for the surface coating industry in the Pearl River Delta region of China, Sci Total Environ, 583, 19-28, 10.1016/j.scitotenv.2016.12.172, 2017.
Zhong, Z., Zheng, J., Zhu, M., Huang, Z., Zhang, Z., Jia, G., Wang, X., Bian, Y., Wang, Y., and Li, N.: Recent developments of anthropogenic air pollutant emission inventories in Guangdong province, China, Sci Total Environ, 627, 1080-1092, 10.1016/j.scitotenv.2018.01.268, 2018.
Zhou, Z., Deng, Y., Zhou, X., Wu, K., TAN, Q., Yin, D., Song, D., Chen, Q., and Zeng, W.: Source Profiles of Industrial Emission-Based VOCs in Chengdu (in Chinese), Environmental Science, 41, 3042-3055, 10.13227/j.hjkx.201912203, 2020a.
Zhou, Z., Tan, Q., Deng, Y., Song, D., Wu, K., Zhou, X., Huang, F., Zeng, W., and Lu, C.: Compilation of emission inventory and source profile database for volatile organic compounds: A case study for Sichuan, China, Atmospheric Pollution Research, 11, 105-116, https://doi.org/10.1016/j.apr.2019.09.020, 2020b.
Zhu, W., Guo, S., Zhang, Z., Wang, H., Yu, Y., Chen, Z., Shen, R., Tan, R., Song, K., Liu, K., Tang, R., Liu, Y., Lou, S., Li, Y., Zhang, W., Zhang, Z., Shuai, S., Xu, H., Li, S., Chen, Y., Hu, M., Canonaco, F., and Prévôt, A. S. H.: Mass spectral characterization of secondary organic aerosol from urban cooking and vehicular sources, Atmospheric Chemistry and Physics, 21, 15065-15079, 10.5194/acp-21-15065-2021, 2021.

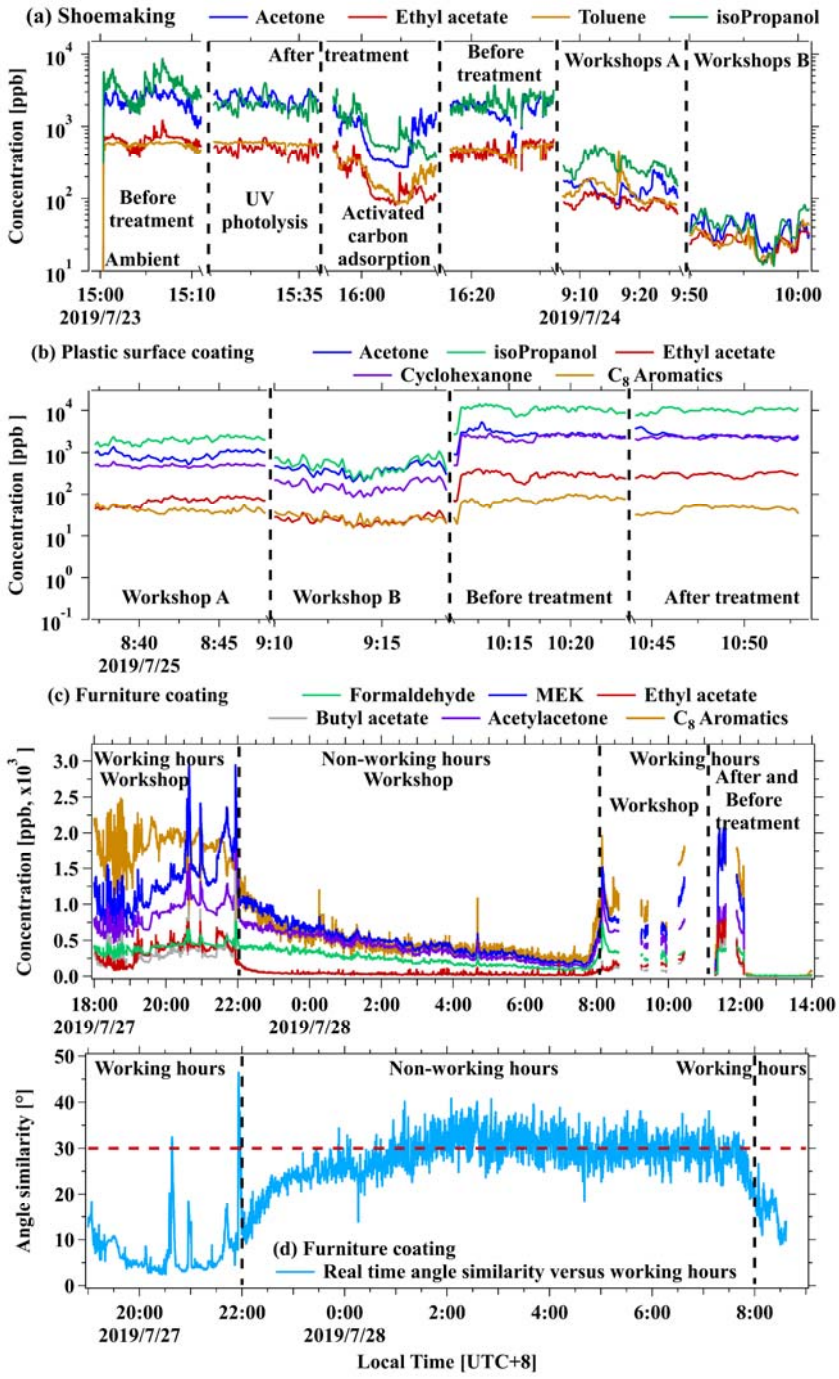

Figure 1. Real-time concentrations of representative ROGs from workshops, before and after the ROG treatment devices in (a) shoe making industry, (b) plastic surface coating industry, and (c) during working hours or non-working hours in the furniture coating industry. (d) The θ angles of mass spectra among real-time concentrations versus average concentration during working time (19:00-22:00) in the furniture coating industry.

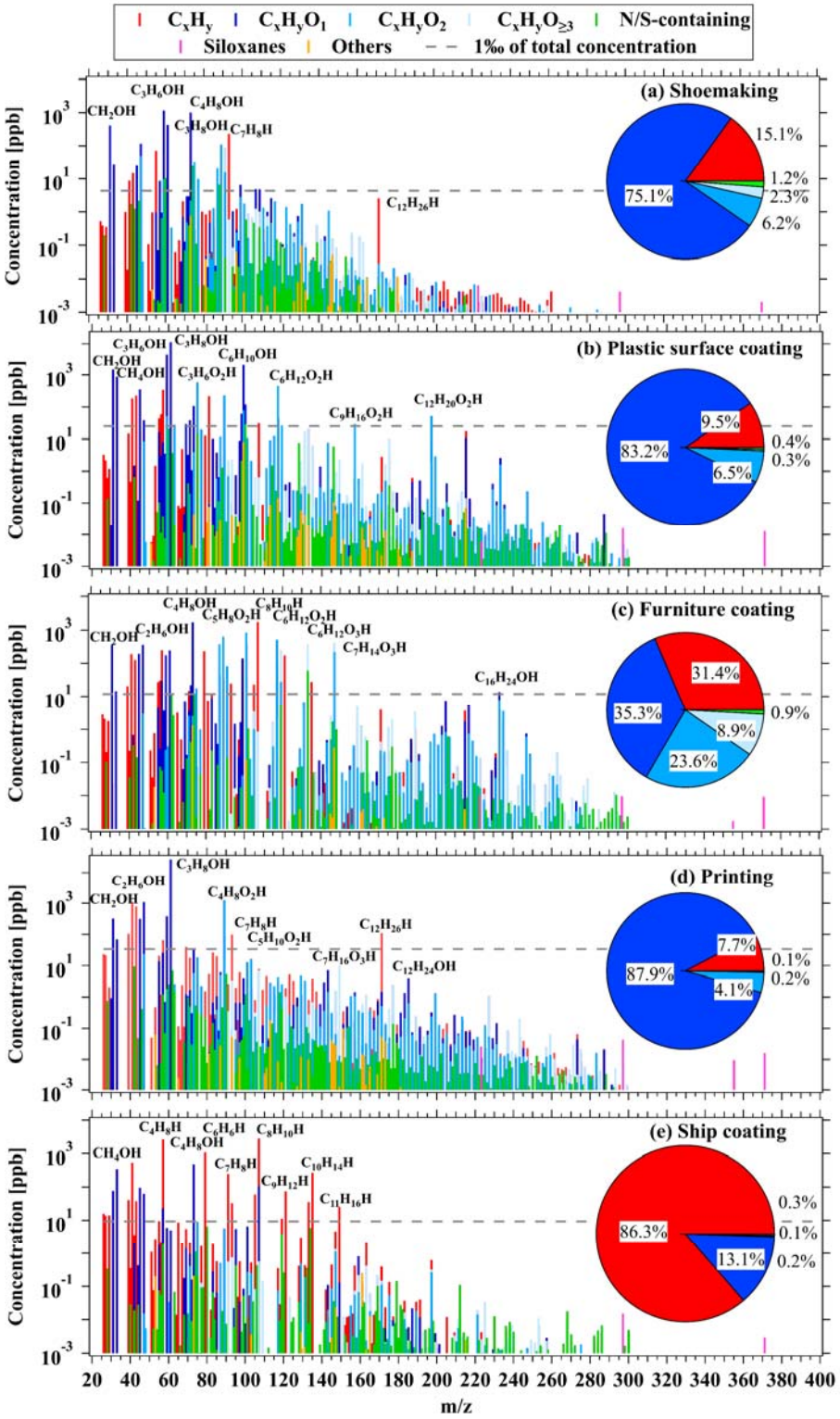

Figure 2. Average concentrations and fractions of ROGs measured by PTR-ToF-MS from stack emissions in (a) shoemaking, (b) plastic surface coating, (c) furniture coating, (d) printing, and (e) ship coating industries.

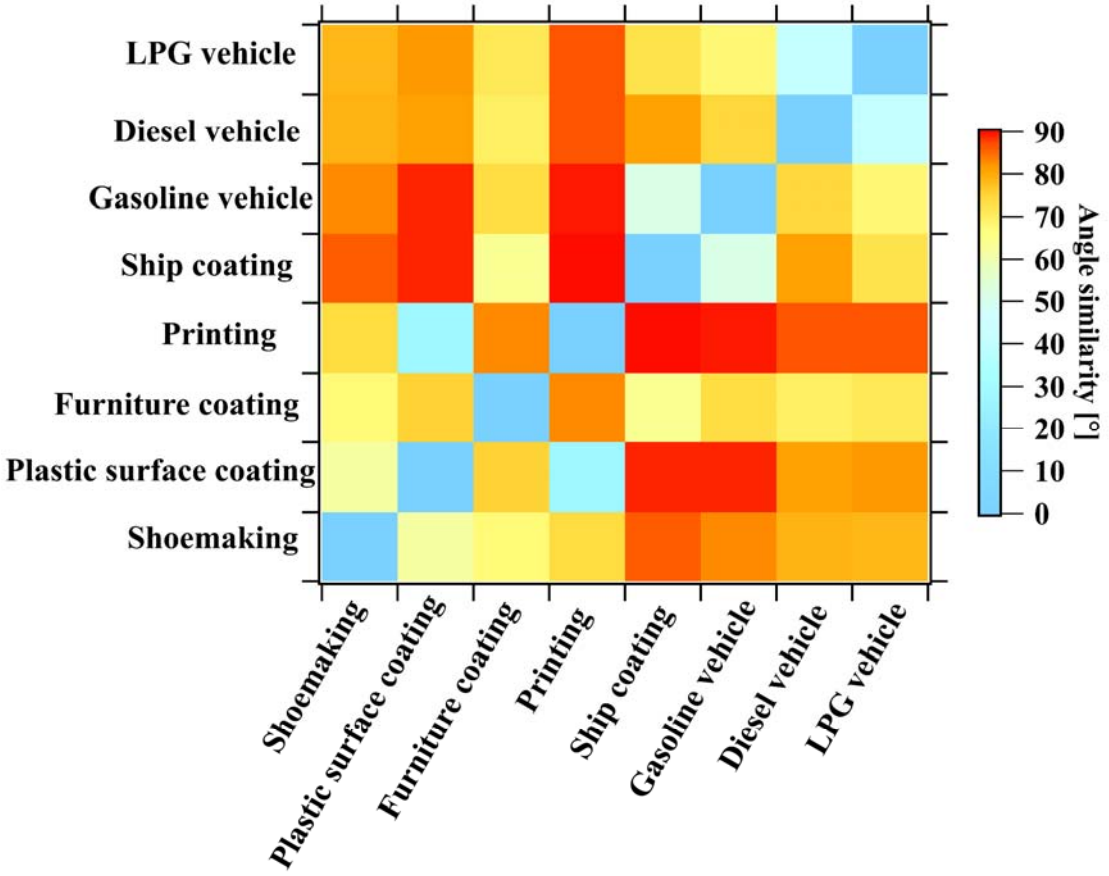

Figure 3. The θ angles among the mass spectra of industrial VCP sources in this study and vehicular emissions from previous study (Wang et al., 2022).

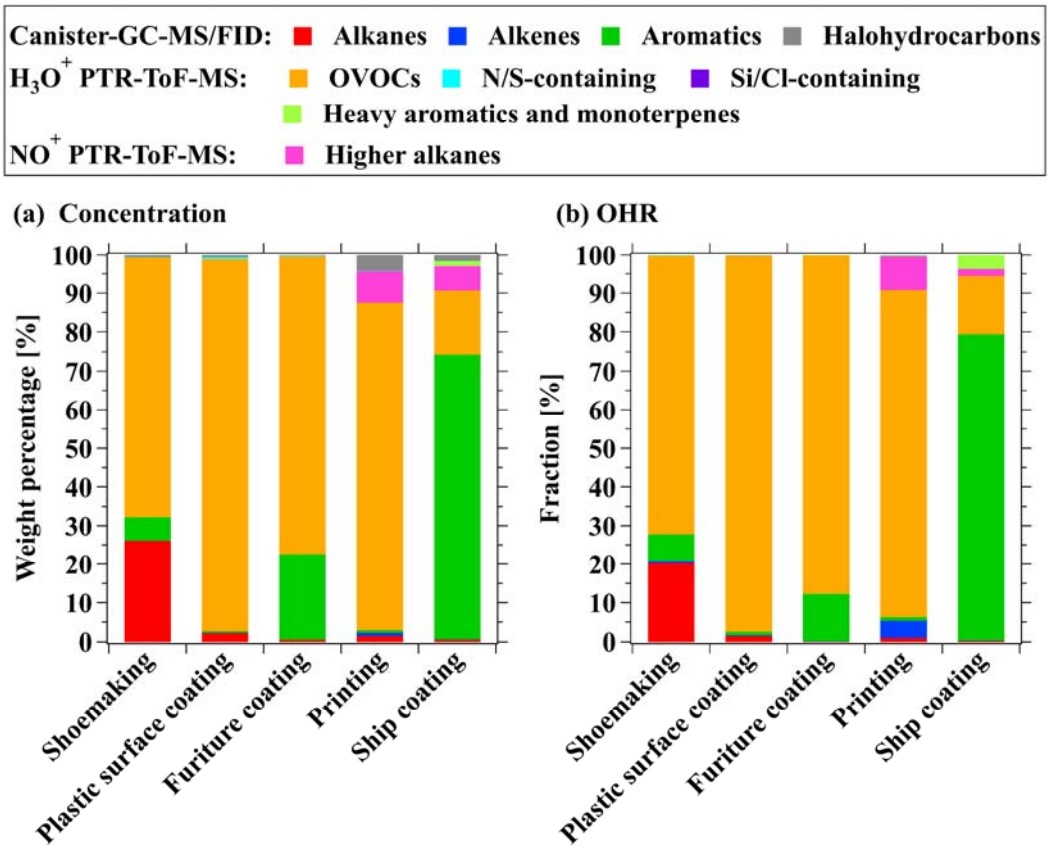

Figure 4. Fractions of (a) concentrations and (b) OHR for ROG components to total ROGs from stack emissions in shoemaking, plastic surface coating, furniture coating, printing, and ship coating industries.

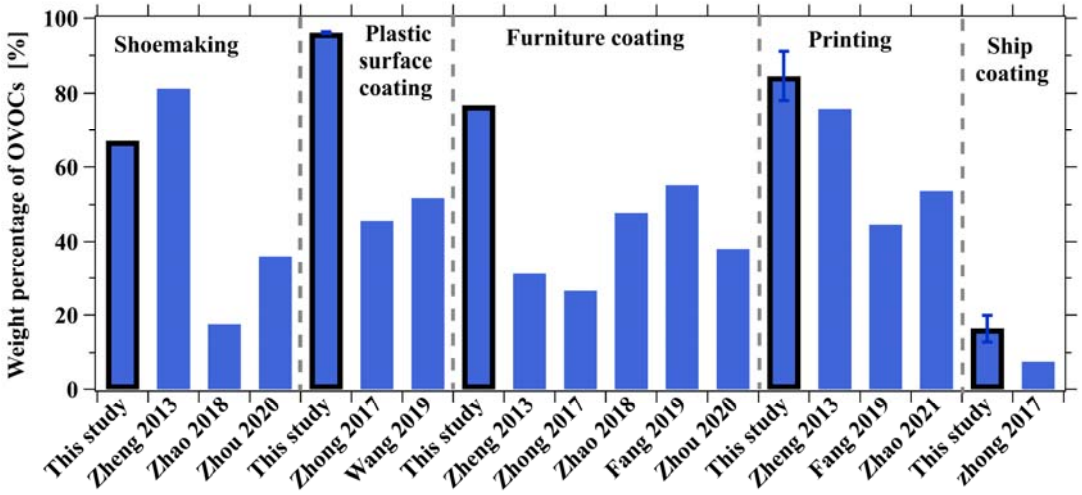

Figure 5. Comparison of OVOC fractions determined from stack emission of industrial VCP sources in this study and those in previous studies. Error bars represent the standard deviations of the weight percentage of OVOCs.

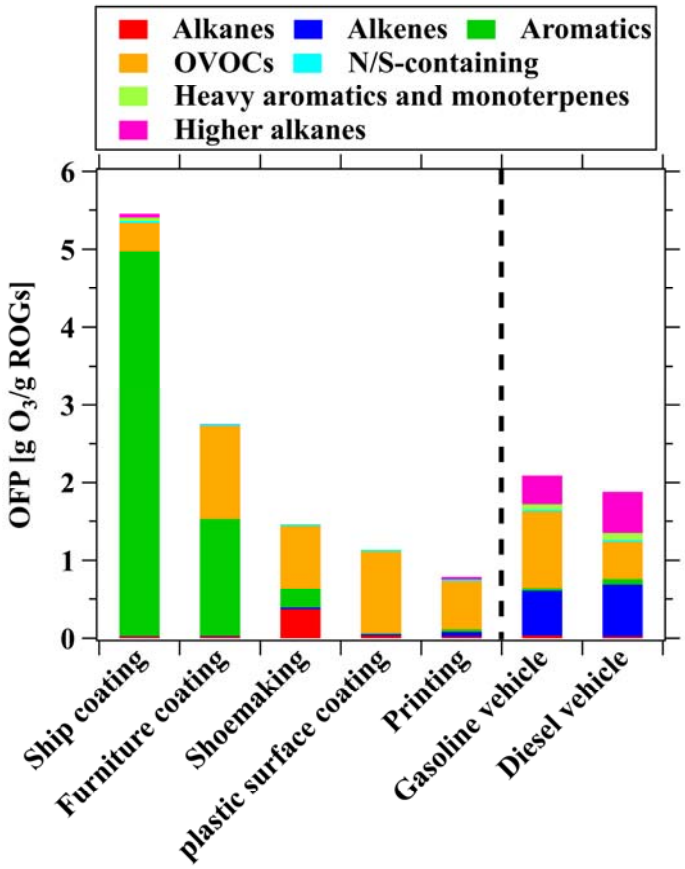

Figure 6. Comparison of OFP among various industrial VCP sources in this study and vehicular emissions from previous study (Wang et al., 2022).

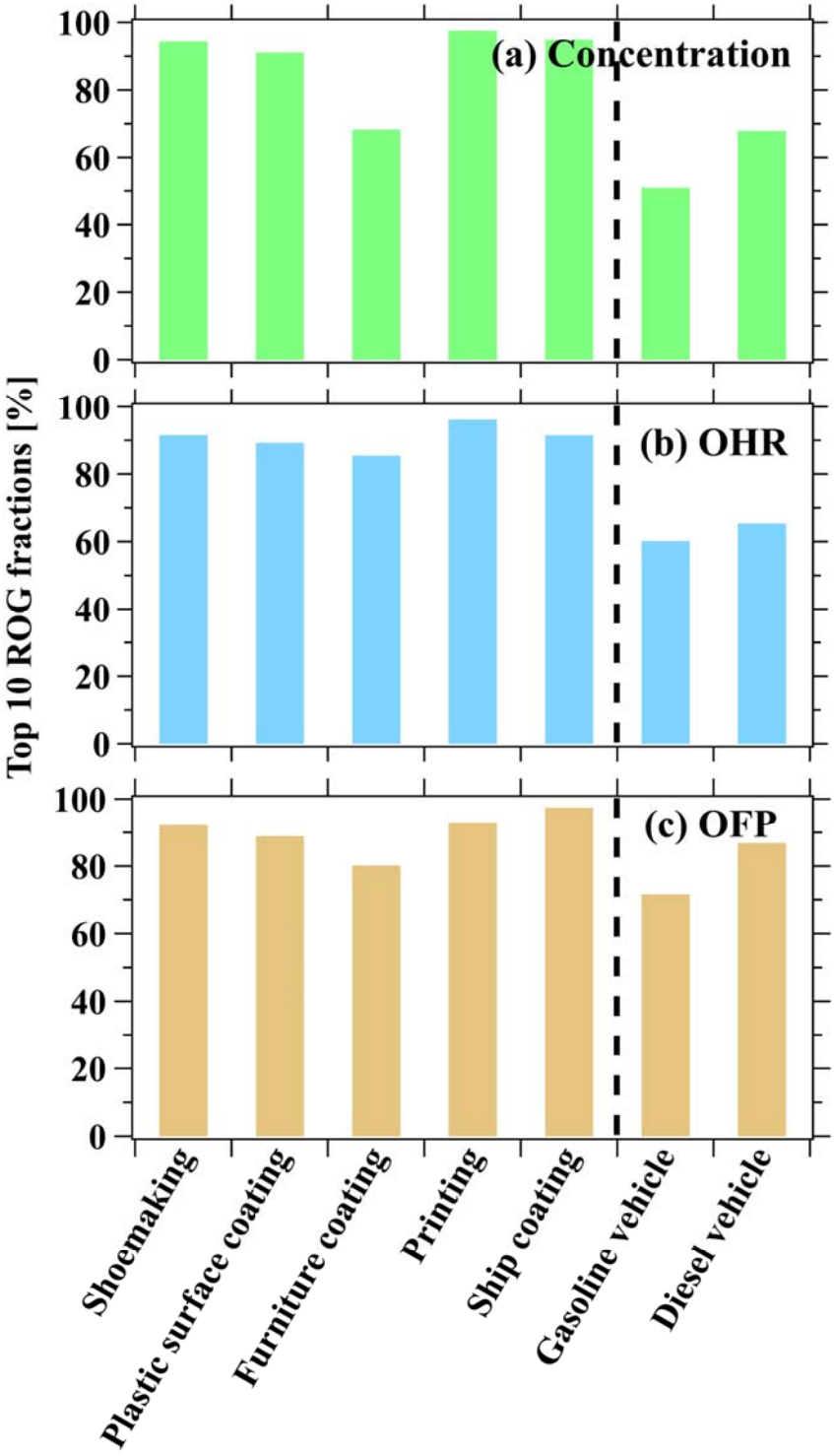

Figure 7. Accumulated fractions of the top ten species in total (a) ROG emissions, (b) OHR, and (c) OFP from industrial VCP sources in this study and vehicular emissions from previous study (Wang et al., 2022).

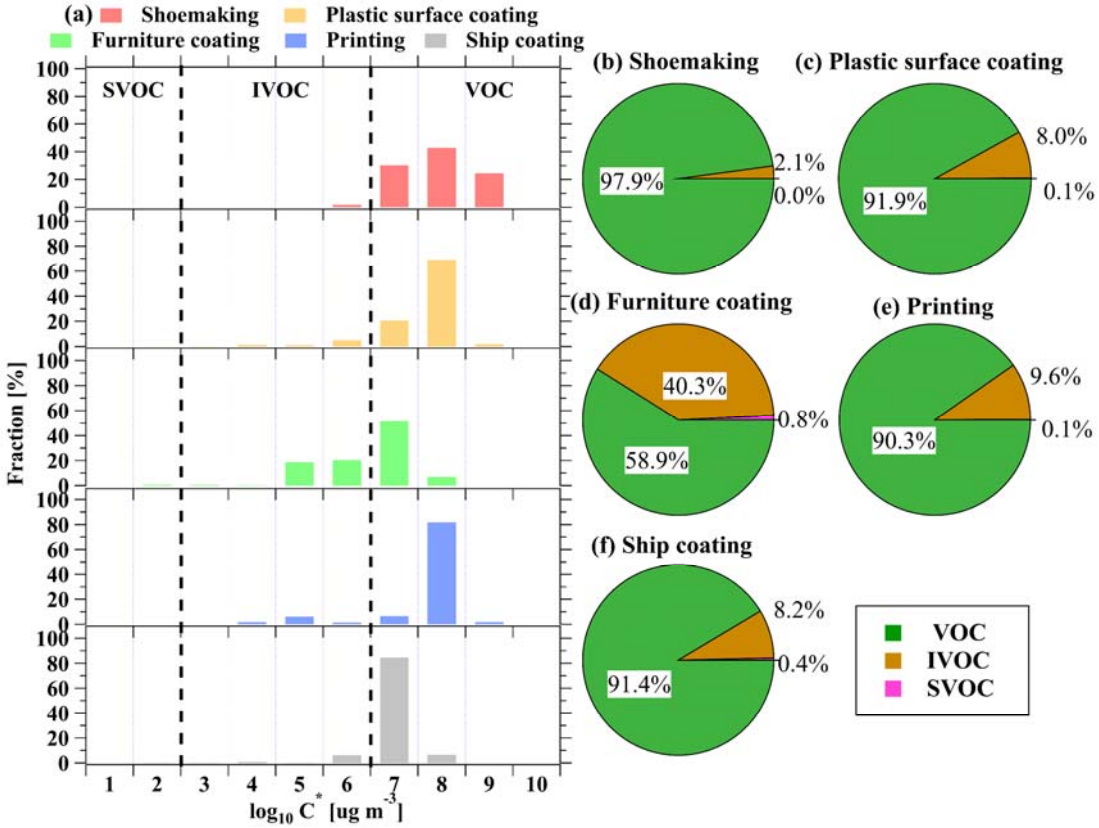

Figure 8. (a) Volatility-binned fractions from stack emissions of various industrial VCP sources, and volatility-binned fractions from different ROG categories in (b) shoemaking, (c) plastic surface coating, (d) furniture coating, (e) printing, and (f) ship coating industries.

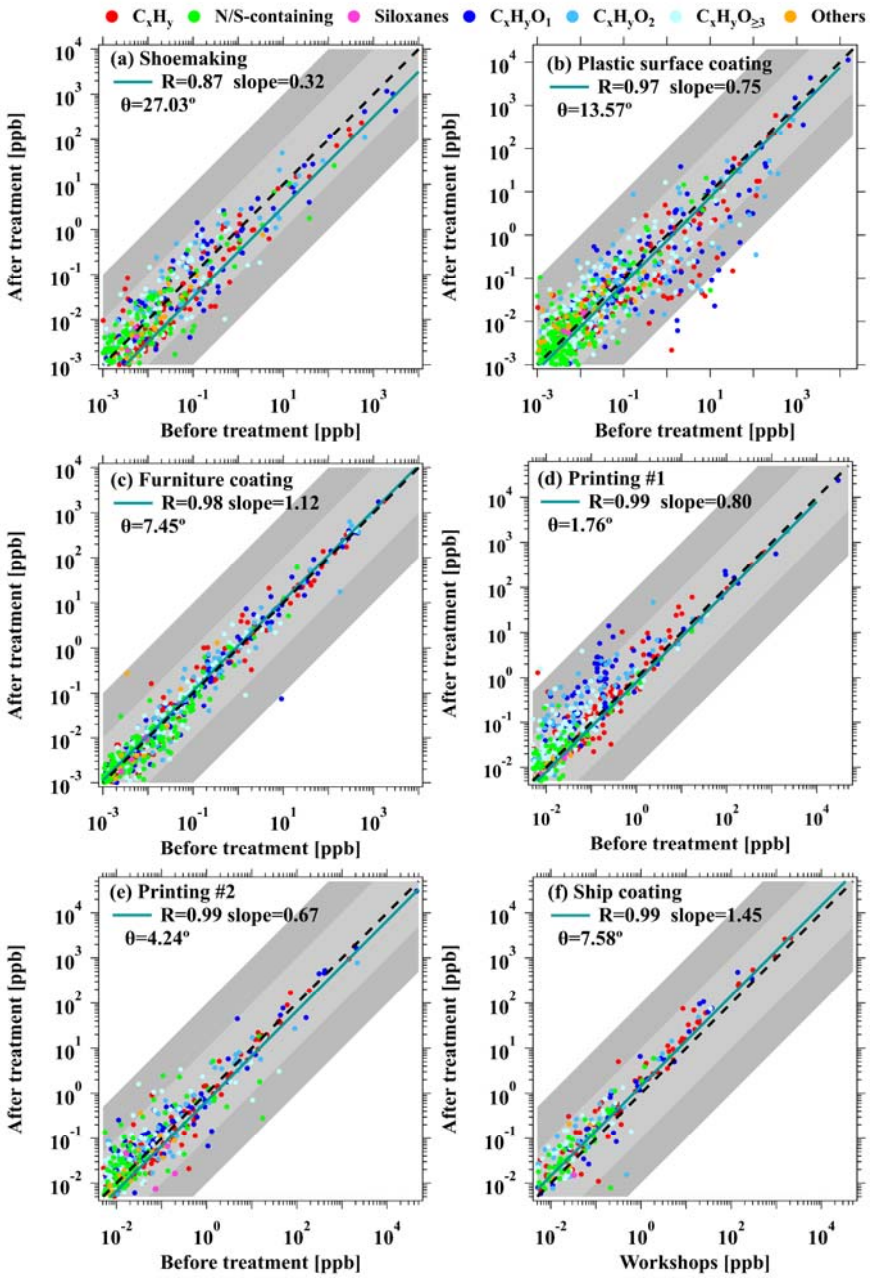

Figure 9. Scatterplots of ROG concentrations between before and after treatment with activated carbon adsorption + UV photolysis in (a) shoemaking, (b) plastics surface coating, (c) furniture coating, and (d) printing industries. Scatterplots of ROG concentrations between before and after treatment with catalytic combustion in (e) the printing industry, and ROG concentrations between workshops and after treatment with catalytic combustion in (f) the ship coating industry. The green lines are the fitted results for all data points. The black dashed lines represent 1:1 ratio, and the shaded areas represent ratios of a factor of 10 and 100.

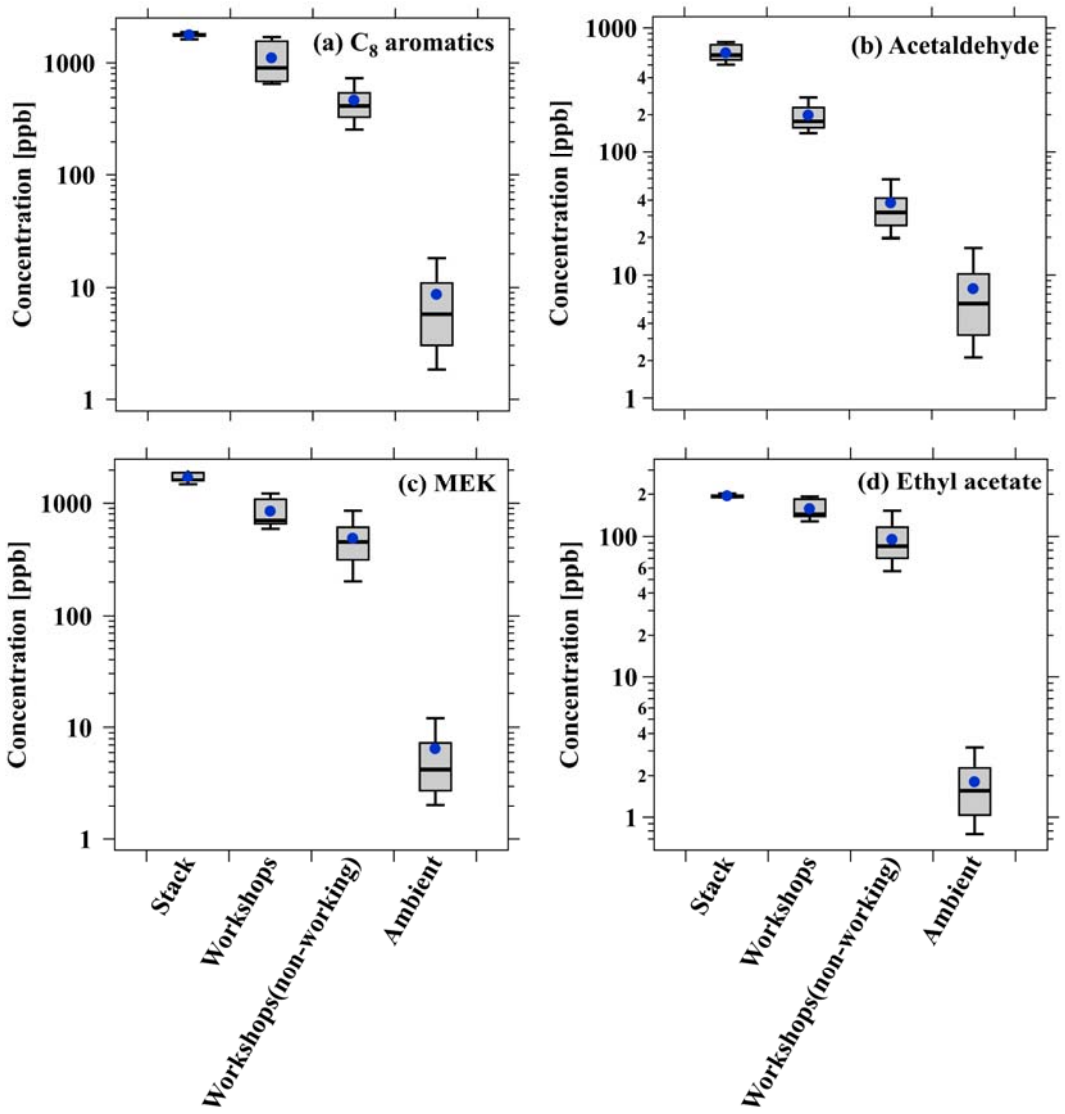

Figure 10. Boxplots of (a) C_8 aromatics, (b) acetaldehyde, (c) MEK, and (d) ethyl acetate concentrations across the stack, workshops during working and non-working hours in the furniture coating industry, and ambient measurement near the industry, respectively.

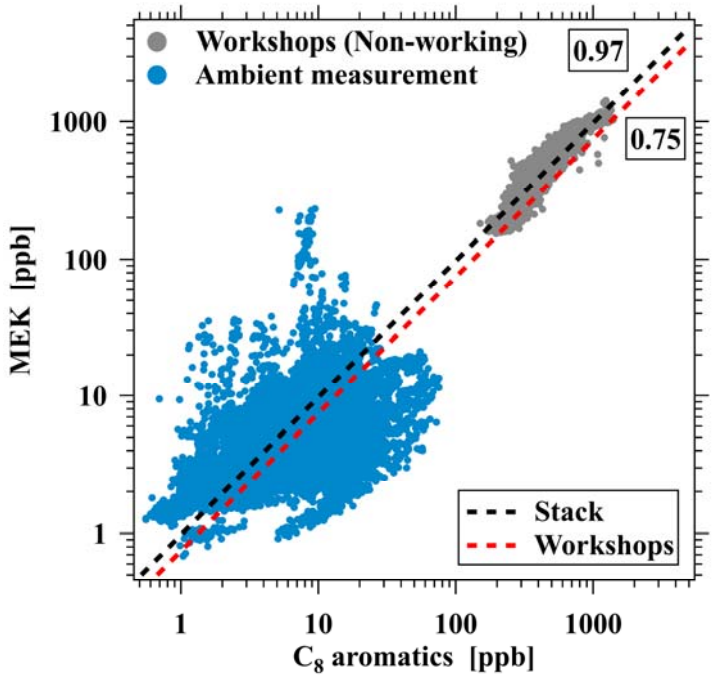

Figure 11. Scatterplot of MEK versus C_8 aromatic concentrations from workshops during non-working hours in the furniture coating industry and ambient measurement near the industry. The black and red dashed line represent ratios of ROG pairs for stack and workshops emission in furniture coating industry.